TRC1606

Estimating Camber, Deflection, and Prestress Losses in Precast, Prestressed Bridge Girders

Ahmed Almohammedi
W. Micah Hale

Department of Civil Engineering
University of Arkansas in Fayetteville
Fayetteville, AR 72701

Final Report

August 2019

TRC1606

Estimating Camber, Deflection, and Prestress Losses in Precast, Prestressed Bridge Girders

Ahmed Almohammedi
W. Micah Hale

Department of Civil Engineering
University of Arkansas in Fayetteville
Fayetteville, AR 72701

Final Report

August 2019

Disclaimer:
This report represents the views of the authors, who are responsible for the factual accuracy of the information presented herein. The views expressed here do not necessarily reflect the views of the Arkansas Department of Transportation.

1. Report No. TRC1606	2. Government Accession No.	3. Recipient's Catalog No.
4. Title and Subtitle Estimating Camber, Deflection, and Prestress Losses in Precast, Prestressed Bridge Girders		5. Report Date: August 2019 6. Performing Organization Code:
7. Author(s) Ahmed Almohammedi and W. Micah Hale		8. Performing Organization Report No.
9. Performing Organization Name and Address Department of Civil Engineering University of Arkansas in Fayetteville Fayetteville, AR 72701		10. Work Unit No. 11. Contract or Grant No.
12. Sponsoring Agency Name and Address Arkansas Department of Transportation, Transportation Research Committee 10324 I-30, Little Rock, AR 72209		13. Type of Report and Period Final Report 14. Sponsoring Agency Code
15. Supplementary Notes Supported by a grant from the Arkansas Department of Transportation		

16. Abstract

Many medium and long precast prestressed concrete girders have camber less than the design values. This discrepancy between the design and the actual camber creates construction problems during installing the cast-in-place concrete deck. The objective of this project is to improve the accuracy of estimating long-term camber, deflection, and prestressed losses of precast, prestressed concrete girders.

The experimental program consisted of measuring the concrete properties and performing field measurements for camber, deflection, and prestress losses for girders in AR. The investigation involved testing nine full-scale girders from two prestressed concrete plants that regularly supply concrete girders to bridge projects in Arkansas. In the project, nine full scale prestressed concrete girders including AASHTO Type II, III, IV, and VI girders were instrumented. Camber and deflection were measured for several girders from each type.

Field measurements and the laboratory testing shows that the current method that the ARDOT uses overestimates camber, specifically in the AASHTO Type II and III girders. The measured camber at erection for all girders was less than the design camber by 93%, 128%, and 25% for AASHTO Type II, III, and VI girders, respectively. The over estimation in camber is mainly attributed to the actual concrete compressive strength at release being greater than the specified compressive strength which was as high as 73% for some girders. It was also determined that the 2014 AASHTO LRFD Refined Method of estimating prestress losses overestimates the total prestress losses at the time of deck placement for the AASHTO Type II and III girders.

17. Key Words	18. Distribution Statement
Camber, Deflection, Prestress losses, Precast Prestressed concrete girder, Modulus of elasticity, Creep, Shrinkage.	None.

19. Security Classif. (of this report)	20. Security Classif. (of this page)	21. No. of Pages	22. Price: N/A
Unclassified	Unclassified	86	

Table of Content

LIST OF FIGURES

LIST OF TABLES

ACKNOWLEDGMENTS

We would like to thank the Arkansas Department of Transportation for sponsoring this research project. The authors would like to thank the two precast concrete plants; Coreslab Structures Inc., Tulsa, OK and J.J. Ferguson Prestress-Precast Co., Inc., Greenwood, MS for their participation and cooperation in this project. Special thanks are due to Mr. Rick Stanley and Mr. Chris McKenney at ARDOT, Mr. Neil Drews at Coreslab Structures Inc., Mr. Patrick Stevens at BGE Inc. and Mr. Glenn Brooks at J.J. Ferguson Prestress-Precast Co., Inc.

CHAPTER ONE:

Introduction

1.1 Introduction

Most short and medium span bridges in the United States are built with either precast, prestressed concrete girders or steel girders. The design of precast, prestressed concrete girders causes an upward deflection, or camber, at mid-span of the girder. During fabrication, the steel strands are tensioned between two abutments, and then the concrete is placed. When the concrete achieves the required compressive strength, the strands are cut, and the force from the strands is transferred to the hardened concrete. This transfer of prestress force creates a bending moment, which results in an upward deflection of the girder, creating camber. Accurate prediction of camber is essential especially during fabrication of cast-in-place bridge decks. If the camber at erection is much less than the design value, the deck thickness must be increased, and this adds extra dead load, which was not accounted for in the design. If the camber is more than the predicted value, the top flange of the girder may interfere with the deck reinforcement. In both cases, the deck profile may have to be redesigned. This can lead to changes in the construction plans, which may delay the project and increase the project's cost.

Release camber, which occurs when the prestressing strands are detensioned, depends mainly on the concrete material properties, strand stress, girder length, and girder cross section. This camber is calculated based on elastic beam theory. If the material properties and the strand stress are predicted accurately, the release camber can also be accurately predicted (Tadros et al., 2011). The release camber, or the instantaneous camber, is used in many design methods to estimate camber at the time of girder erection (PCI design handbook 2010). The erection camber is affected by the time-dependent deformation of the concrete, namely; creep and shrinkage. Creep and shrinkage shorten the girder over time which reduces the force in the strands. This loss in the prestressing force, along with strand relaxation loss, is time-dependent and also affects camber growth and magnitude (Nilson 1987).

1.2 Problem Statement

The AASHTO LRFD Bridge Specifications do not explicitly give design procedures for estimating the camber of precast prestressed concrete girders. The multipliers methods of the PCI Design Handbook are widely used to predict the long-term camber and deflection due to its simplicity. However, using the multiplier methods have resulted in differences between the design camber and the actual camber (Stallings and Eskildsen 2001). In most cases, girders arrive at the bridge site with camber much less than the design value (Tadros et al., 2011). Consequently, the deck thickness is increased, adding extra dead load, which was not accounted for in the original design. Insufficient camber requires increasing the haunch thickness which in some cases increases the overall deck thickness rather than the concrete along the girder length. The haunch is the additional thickness of concrete between the top flange of the girder and the bottom of the deck. The haunch is designed to accommodate for small differences in camber curvature along the girder. Differences between the design camber and the actual camber require additional work and time to adjust the cast-in-place bridge deck elevations and to maintain the roadway profile requirements. The problem can be more complicated when the variability in camber occurs between girders of the same span in a bridge rather than a consistence difference in all girders. Therefore, inaccurate prediction of camber at girder erection can increase the cost, delay the project, and cause construction-related problems. Inaccurate camber prediction also means the deflection is also not correct since both camber and deflection are affected by the same factors. An accurate prediction of camber and deflection is essential to prevent large deflections caused by the deck weight. Noticeable deflection or sag in the bottom of the girders may cause serviceability issues and raise public concern.

Factors influencing camber and deflection are time dependent and related to each other, making an accurate prediction of camber trend challenging (PCI Bridge Design Manual, 2014). The initial camber is influenced by the modulus of elasticity of the concrete and strand stress at the time the prestressing force is released. The camber at erection, on the other hand, is influenced by concrete creep and shrinkage, prestress losses, and various factors associated with the difference in quality-control and storage conditions or the variation in the ambient temperature and humidity. The magnitude of creep strain is also determined by the concrete

strength at release (ACI Committee 209R-92, 2008). For an accurate prediction of camber and deflection, an appropriate estimate for all the influential factors is necessary, and this can be a complicated task during the design stage.

1.3 Research Objectives and Methodology

The objective of this research is to improve the accuracy of estimating long-term camber, deflection, and prestressed losses of precast, prestressed concrete girders. The experimental program consisted of concrete materials testing and field measurements for camber, deflection and prestress losses. The investigation involved instrumenting and testing nine full-scale girders from two prestressed concrete plants that regularly supply concrete girders to bridge projects in Arkansas. Seven girders were fabricated at Coreslab Structures Inc. in Tulsa, OK and two girders were cast at J.J. Ferguson Prestress-Precast Co., Inc. in Greenwood, MS. Different girders cross sections of various spans were included to obtain data on a variety of girders used in ARDOT bridges. AASHTO Types II, III, IV, and VI girders were all examined in this project. These girders were used in the construction of three bridges in Arkansas.

The research project was composed of five tasks. In **Task One**, the fresh and hardened concrete properties were measured for all girders. This allowed the research team to determine the actual material properties of the concrete used to cast the girders. This included measuring concrete properties at the precast facility and also casting specimens at the facility and then later testing the concrete at the University of Arkansas' research laboratory. The laboratory testing included compressive strength, modulus of elasticity, unit weight, creep, and shrinkage. **Task Two** focused on measuring the change in strain and temperature of the prestressing strands within the girders. Strain was recorded for each of the nine girders prior to strand release and continuing through deck placement. Vibrating wire strain gauges were used to measure the strands' strain. In **Task Three,** camber was measured and monitored for several of the girder types. Like the strain measurements, camber was measured prior to strand release and continued through deck placement. **Task Four** examined the effect of coarse aggregate stiffness on the prediction of modulus of elasticity. The final report will be prepared in **Task Five**.

CHAPTER TWO:

Literature Review

1.4 Introduction

Several state departments of transportations have investigated camber variability and updated their prediction methods based on their research findings (Honarvar et al., 2015), (O'Neill and French, 2012), (Rizkalla et al., 2011), (Rosa et al., 2007). Each state developed its own method or modified the basic procedures. A single design approach that quantifies camber behavior would not be accurate to predict camber for girders cast in any precasting plant, because camber is affected by concrete properties which are affected by the local materials. The properties of these local materials can affect concrete modulus of elasticity, shrinkage, and creep (O'Neill and French, 2012; Cook et al., 2005). Moreover, concrete strength at release, curing time, and curing method are also different between plants and these also affect concrete properties. Even storage time and method of girder storage influence camber growth (Tadros et al., 2011). For this project, modifications to the current design methods for long-term camber and deflection of the precast prestressed concrete girders used by ARDOT are proposed (ARDOT).

This chapter provides a summary of some previous research conducted on camber prediction. Methods to predict modulus of elasticity, shrinkage, and creep of concrete are also discussed in this chapter. Discussion of prediction methods for prestress losses are also presented.

1.5 Summary of Previous Research

1.5.1 Martin (1977)

In 1977, Martin suggested a method to estimate erection camber and deflection, known today as Martin Multipliers. The 2010 PCI Design Handbook adopted this method for estimating long-term camber and deflection which is called *The Multipliers Method*. It is also presented in the PCI Bridge Design Manual. To estimate camber at girder erection, Martin suggested multiplying the camber due to the prestressing force by 1.8 and multiplying the deflection due to self-weight by 1.85. This method was based on a very general assumption regarding concrete

properties, prestress losses, and concrete age at erection. Martin assumed that one-half of the long-term camber, deflection, and prestress losses occurs by the time of erection which he assumed was 30 to 60 days from casting the girder. These assumptions can result in differences between the proposed multipliers method and the actual camber (Tadros et al., 2011) (Honarvar et al., 2015). Although Martin recommended using other camber prediction methods for more accurate results, many design engineers and software still use Martin's method due to its simplicity.

1.5.2 Tadros et al. (2011)

Tadros et al. (2011) examined camber variability in prestressed concrete girders and recommended a detailed method to estimate the initial and long-term camber. This method was limited to conditions up to and including the application of the deck. The proposed method implemented the 2005 AASHTO LRFD Bridge Design Specifications formulas for predicting prestress losses, modulus of elasticity, creep, and shrinkage into a spreadsheet to calculate the initial and long-term camber. For the initial camber estimation, Tadros et al. considered the effect of strand debonding, storage condition (girder overhanging length), friction at girder ends, and the accuracy of estimating modulus of elasticity and prestress losses on the initial camber prediction. For the long-term camber, the proposed method considered the elastic deflection due to the long-term prestress loss between prestress release and time of deck placement. The initial prestress is assumed to be constant with time. An aging coefficient of 0.7 times the creep coefficient was used to estimate the reduction in prestress force due to creep.

Tadros et al., (2011) recommended considering local material properties, storage conditions, and construction practices to better predict camber but also allowing for 50% variability in camber. The author proposed using the detailed method of the AASHTO LRFD Bridge Design Specifications to predict long-term prestress loss due to creep and shrinkage of the concrete and relaxation of the prestressing steel.

1.5.3 Rosa et al. 2007

In 2007, Rosa et al., conducted a study aimed to improve camber prediction by modifying the current methods used by Washington State Department of Transportation. The study included material testing and analysis of field measurements. The author measured the camber at release and before the eight girders were shipped. Compressive strength, elastic modulus, creep and shrinkage were measured on representative samples. Results from measuring camber and concrete properties were used to evaluate the current camber prediction methods included in AASHTO LRFD Bridge Design Specifications. The author recommended adjustment factors of 1.15 to the modulus of elasticity of concrete estimated by the AASHTO LRFD Bridge Design Specifications. A computer program was developed to predict camber over time. The program was calibrated for the initial camber using the release camber for 146 girders. The computed long-term camber was compared with camber for 91 girders measured at erection. The author did not measure strand stress but did refer to the significant effect of prestress losses on camber. The study did not include measurements for the erection camber and deflection due to deck weight or the effect of environmental conditions on camber prediction.

1.5.4 Honarvar et al. 2015

Honarvar et al. (2015) conducted a study to improve the accuracy of camber prediction in prestressed concrete girders. The author measured the compressive strength, elastic modulus, creep, and shrinkage strain for four high strength concrete (HSC) and three NC (normal strength concrete) mixtures where represented concrete used at three precast plants. The release camber was measured using string potentiometers, but most of the camber measurements were collected from the precasting plant's database. The long-term camber was measured for 66 prestressed concrete girders during storage and at the time of erection at the site. The author proposed deferent multipliers for the long-term camber based on field measurements and the collected camber values. The author concluded that the 2010 AASHTO LRFD Bridge Design Specifications formulas for modulus of elasticity, creep, and shrinkage provided the best estimate when compared to the measured values. The study revealed that the measured release strength was 10% to 40% higher than the design values. The elastic shortening loss and the long-term

prestress losses were not measured in the field, but the authors referred to the effect of prestress losses on camber at release and at the time of girder erection. Deflection due to the cast-in-place deck was not measured because the focus of the study was on the camber up to the time of girder erection.

1.5.5 O'Neill and French, 2012

O'Neill and French (2012) published a report sponsored by Minnesota Department of Transportation which investigated the accuracy of estimating camber and deflection in prestress concrete girders. The authors collected historical data from two plants, and this historical data included data for compressive strength and camber at release and at erection. The study also included instrumenting fourteen girders using a stretch-wire system to monitor camber change from strand release to girder shipment. Based on the collected data, the design camber at release and at erection was 26% and 16.5% less than the measured camber, respectively. The authors explained that the main cause for these discrepancies was the high compressive strength at release. The compressive strength at release was 15.5% to 35% greater than the design strength. The study concluded with recommendations to increase the specified release compressive strength by 15% and use ACI 318-08 and AASHTO LRFD Bridge Design Specifications 2010 equations to predict the modulus of elasticity of concrete. Additional findings included that the thermal effect decreased the prestressing force by 3%, on average. The report did not include measurements for the girder's deflections due to deck weight.

1.5.6 Cook et al. 2005

Florida Department of Transportation (FDOT) sponsored a study to evaluate and calibrate its camber prediction design software called FDOF LFRD PSBeam v.1.85. The study involved measuring the camber for 13 girders which included 78-inch Florida Bulb Tee Girders, AASHTO Type IV, and AASHTO Type V Girders. Camber was measured at release and periodically over 6 months. Concrete was sampled to obtain compressive strength and modulus of elasticity values in conjunction with the field measurements. Camber measurement results indicated that the design program, used by FDOT at that time of the study, overestimated camber by 45 to 75% for

the 78-inch Bulb Tee Girder and by 50% for the AASHTO Type IV Girder. The study also investigated the effect of using granite and Florida Limerock as a coarse aggregate on long-term camber growth. However, it would be more realistic to relate the effect of coarse aggregate type to the modulus of elasticity or creep of concrete. Measurements for the long-term prestress losses were not present in the study which, if performed, may explain the reasons for the differences between the design and the actual camber.

1.6 Initial Camber Prediction

In most design practices, the initial camber is calculated by assuming linear elastic behavior for the girder (PCI Design Handbook, 2010). The upward deflection due to the prestressing force is calculated and then subtracted from the downward deflection due to member self-weight. The accuracy of this procedure for predicting initial camber depends mainly on the accuracy of estimating concrete material properties and the force in the prestressing strands after release. Accurate estimation of the initial camber during design requires careful an accurate prediction of the concrete modulus of elasticity, unit weight, and initial prestress losses.

The upward deflection due to the initial prestressing force is calculated using equations based on the strand patterns and the number of hold-down points (harps), if any. The most common strands pattern used by ARDOT is two groups of straight strands at the top and at the bottom of the girder. The equation below can be used for the straight strand profile and for two points draped profile. The Design Aid 15.1.4 of the 2010 PCI Design Hand Book provides equations for calculating the upward component of camber for different strands patterns.

The initial camber can be determined by calculating the upward deflection due to prestressing force as follow:

$$\uparrow V_{prestress} = \frac{P_i L^2}{8 E_{ci} I_i}(e_c - (e_e - e_c)\frac{4X^2}{3L^2} \qquad (2\text{-}1)$$

The downward deflection due to self-weight is given as:

$$\downarrow V_{sw} = \frac{5 w_{sw} L^4}{384 E_{ci} I_c} \qquad (2\text{-}2)$$

The initial camber is then calculated as follows:

$\Delta_{\text{Initial camber}} = \uparrow\Delta_{\text{prestress}} - \downarrow\Delta_{\text{self-weight}}$

Where:

P_i = initial prestressing force immediately after transfer

e_m = strand eccentricity at the center of the member

e_e = strand eccentricity at the ends of the member

L = girder span between supports

E = modulus of elasticity of the concrete at transfer

I = moment of inertia

w_{sw}= linearly distributed self-weight load

x = distance from the end of the member to the point of hold down.

1.7 Long-term Camber Prediction Methods:

1.7.1 Multiplier Method

There is no specific method to predict long-term camber in the 2014 AASHTO LRFD Bridge Design Specifications. The PCI Bridge Design Manual provides a set of multipliers in Table 8.7.1-1 reprinted here in Table 2-1 due to its popularity in camber prediction. Most state department of transportations and design software use multipliers to estimate the long-term camber due to its simplicity. To estimate camber at girder erection, the deflection from the member weight is multiplied by 1.85 and the up-ward camber from the prestressing force is multiplied by 1.8. Then the erection camber is calculated by subtracting the deflection as shown in Eq. (2-3). These multipliers provide a guide or approximate estimate for the long-term camber. The method was developed based on general assumptions of concrete properties and construction/fabrication practices as stated in section (2.2.1).

$$\Delta_{\text{erection camber}} = 1.8\,(\uparrow\Delta_{\text{prestress}}) - 1.85\,(\downarrow\Delta_{\text{self-weight}}) \qquad (2\text{-}3)$$

Final camber at the end of the bridge's service life can be estimated in the same way as the erection camber by using the suitable multipliers from Table 2-1 and adding components for any additional dead loads.

Table 2-1. Multipliers for estimating long-term camber and deflection.

Camber at Erection	Without Composite Deck	With Composite Deck
Deflection (↓) component − apply to the elastic deflection due to the member weight at release of prestress	1.85	1.85
Camber (↑) component − apply to the elastic camber due to prestress at the time of release of prestress	1.8	1.8
Deflection (↓) component − apply to the elastic deflection due to the member weight at release of prestress	2.7	2.4
Camber (↑) component − apply to the elastic camber due to prestress at the time of release of prestress	2.45	2.2
Deflection (↓) component − apply to elastic deflection due to superimposed dead load only	3	3
Deflection (↓) component − apply to elastic deflection caused by the composite topping	--	2.3

Source: (2014 PCI Bridge Design Manual, Table 8.7.1-1)

1.7.2 Improved Multiplier Method:

A revised set of multipliers were proposed to improve the accuracy of the method (Tadros et al., 1985). The proposed set of multipliers allows one to use the actual creep coefficient and prestress losses. Also, it takes into account the girder deflection due to prestress losses. This method is presented in the PCI (2010) Bridge Design Handbook in Table 8.7.2-1 as the Improved Multiplier Method. From this method, Equations (2-4) and (2-5) are used to predict camber at girder erection and at an arbitrary final time, respectively.

$$\Delta_{erection} = \uparrow\Delta_{prestress}\,(1 + C_a) - \alpha\,(1+\chi\,C_a)\downarrow\Delta_{p.loss.} - (1+C_a)\downarrow\Delta_{self\ w.} - (1)\downarrow\Delta_{dead\text{-}load} \qquad (2\text{-}4)$$

$$\Delta_{final} = \uparrow\Delta_{prestress}\,(1 + C_u) - \alpha\,(1+\chi\,C_a)\downarrow\Delta_{p.loss.} - (1+C_u)\downarrow\Delta_{self\ w.} - (1+C'_u)\downarrow\Delta_{dead\text{-}load} \qquad (2\text{-}5)$$

Where:

C_a = creep coefficient for loading applied immediately after transfer and strains measured at time of erection. Average value is 0.96.

C_u= ultimate creep coefficient for loads applied immediately after transfer. Average value is 1.88.

C_u'= ultimate creep coefficient for loads applied at time of erection. Average value is 1.50.

α = time-dependent prestress loss at erection divided by total time-dependent prestress loss. Average value is 0.60.

χ = Bazant's aging coefficient. Average value is 0.70.

$\Delta_{dead\text{-}load}$: deflection due to dead load. If there is a dead load on the plain and composite stages, both must be considered.

$\Delta_{p.loss.}$ = deflection due to prestress losses.

The ratio of prestress losses at erection to total prestress losses is assumed in the 2010 PCI Design Manual to be 0.6. However, studies have revealed that 90% of the prestress losses occur by the time the cast-in-place deck begins to act compositely with the girder as stated by Tadros et al. (2011). The improved multipliers method is limited to the deflection at the time of deck placement before the composite action between the deck and the girder occurs, because they were developed only for prestressed concrete building members.

1.7.3 Tadros et al. 2011

Tadros et al. (2011) proposed a method to predict long-term camber of prestressed girders limited to the time just before deck placement. The concrete age at release and at deck placement was assumed to be 0.75 and at 120 days, respectively. Two factors were proposed to convert the initial camber at release to the erection camber. The first factor incorporated the effect of creep on the net camber from the initial prestress force and self-weight deflection, and the second factor included the effect of creep on the elastic deflection due to prestress losses. The two multipliers are shown below:

Multiplier for initial prestress plus self-weight = [1 + ψ (120, 0.75)] (2-6)

Multiplier for the prestress loss = [1 + 0.7ψ (120, 0.75] (2-7)

The elastic deflection due to prestress loss is assumed to be the ratio of long-term prestress loss at deck placement to the jacking force times camber from the initial prestressing force as shown in Eq. (2-8). The net long-term camber is then calculated by multiplying the first and the second multipliers by the initial camber and the elastic deflection respectively.

$$\Delta_{elastic,loss} = (\Delta_{ip} (\Delta_{lt} / f_{pi}) \quad (2\text{-}8)$$

1.8 Prestress Losses

According to the AASHTO LRFD Bridge Design Specifications, the prestressing strands are pretensioned to 202.5 ksi prior to strand release. This 202.5 ksi is 0.75% of their ultimate tension strength for Gr. 270, low-relaxation strands. The effective tension force in these strands decreases from the time the strands are tensioned until the end of the service life of the prestressed concrete member. This decrease in strand stress, also known as prestress losses, are divided into instantaneous losses and time-dependent losses. The instantaneous losses include elastic shortening, relaxation, and seating or anchorage slipping. The time-dependent losses are primarily due to creep and shrinkage of concrete in addition to the small magnitude of strand relaxation. The reduction in strand tension decreases the compression stress in the concrete and this affects the moment capacity and time-dependent deformation of concrete (2014 AASHTO LRFD).

The following section will discuss two methods for predicting prestress losses. These methods are the Detailed Estimate Method, and 2014 AASHTO LRFD Refined Estimate Method.

1.8.1 Instantaneous Losses

1.8.1.1 Relaxation Loss

Generally, relaxation loss of prestressing strands is very small when compared with elastic shortening, shrinkage, and creep losses. The 2014 AASHTO LRFD recommends a value of 1.2 ksi for the relaxation loss that occurs during the time period between prestress transfer and deck

placement and 2.4 ksi for the total relaxation loss at the final time. However, there are equations to predict the relaxation loss in the AASHTO LRFD Bridge Design Specification. Because the loss is small in comparison to the other sources of loss, it is widely acceptable to use the above direct numbers to estimate the relaxation loss.

1.8.1.2 Elastic Shortening Losses

When the prestressing strands are cut, the prestressing force transfers to the hardened concrete and shortens the girder instantaneously causing camber. The shortening in the concrete and the bonded strands lose some of the tension. A portion of this loss is offset by a gain in tension due to the girder's self-weight. The elastic shortening loss is dependent on the modulus of elasticity of concrete at the time of release. The elastic shortening loss equation is derived based on the principle of compatibility of strains assuming full bond between the strands and the surrounding concrete. The 2014 AASHTO LRFD Bridge Specifications provides equation (5.9.5.2.3a-1) to calculate elastic shortening losses replicated here as Eq. (2-9).

$$\Delta f_{pe} = \frac{E_p}{E_{ci}} f_{cgp} \tag{2-9}$$

Where:

Δf_{pe} = losses or gains due to elastic shortening or extension at the time of application any loads (ksi)

f_{cgp} = the concrete stress at the center of gravity of prestressing tendons due to the prestressing force immediately after transfer and the selfweight of the member at the section of maximum moment (ksi).

E_p = modulus of elasticity of prestressing steel (ksi)

E_{ci} = modulus of elasticity of concrete at transfer or time of load application (ksi)

(Al-Omaishi et al., 2009b) recommended the direct method to calculate f_{cgp} by applying the prestressing force before release to the transformed-section properties using the following equation:

$$f_{cgp} = P_i \left[\frac{1}{A_{ti}} + \frac{e_{pti}^2}{I_{ti}} \right] - \left[\frac{M_g e_{pti}}{I_{ti}} \right] \tag{2-10}$$

Where:

A_{ti}= transformed cross section area at time of prestress transfer $(in.)^2$

I_{ti}= girder moment of inertia using transformed section at time of prestress transfer$(in.)^4$.

e_{pti}= strand eccentricity measured from the centroid of the transformed section at the time of prestress transfer $(in.)^2$.

M_g= moment at mid-span due to member self-weight (kip-in.)

The 2014 PCI Bridge Design Manual gives equation (Eq. 8.6.7.1-1) to calculate elastic shortening loss.

$$ES = f_{pi} - f_{po} \tag{2-11}$$

Where:

f_{pi} = initial stress immediately before transfer

f_{po} = stress in prestressing steel immediately after release and it is calculated as follow:

$$f_{po} = \frac{f_{pi} + \frac{E_p}{E_{ci}}\frac{M_g e}{I_g}}{1+a} \tag{2-12}$$

α is given as:

$$\alpha = \frac{E_p}{E_{ci}}\frac{A_p}{A_g}\left[1 + \frac{e^2}{\frac{I_g}{A_g}}\right] \tag{2-13}$$

Where:

A_g = area of concrete gross section

I_g: moment of inertia of the girder gross section

Alternatively, elastic shortening loss may be calculated directly using Equation (2-14). This is from the code commentary (AASHTO LRFD 2014 (C5.9.5.2.3a-1) and uses the gross concrete section properties.

$$\nabla f_{pES} = \frac{A_{ps} f_{pbt} (I_g + e_m^2 A_g) - e_m M_g A_g}{A_{ps} (I_g + e_m^2 A_g) + \frac{A_g I_g E_{ci}}{E_P}} \quad (2\text{-}14)$$

1.8.2 Long-Term Prestress Losses

Long-term prestress losses consist of losses due to shrinkage, creep, and strands relaxation. A variety of methods are available to predict these losses with different accuracy and complexity. The following sections illustrate two of the most widely used methods present in the 2014 AASHTO LRFD.

1.8.2.1 Approximate Estimate of Time-Dependent Losses

Equation 5.9.5.3-1 of the 2014 AASHTO LRFD Bridge Design Specifications provides an estimate for the total losses in the prestressing force at final time due to the effect of creep, shrinkage, and relaxation. This method is derived for normal weight concrete and assumes average humidity and temperature exposure. The equation has three terms which corresponds to creep, shrinkage, and relaxation losses respectively as given in Eq. (2-15). The approximate method estimates time-dependent prestress losses for the standard precast prestressed concrete I-beams and inverted tee sections with composite decks only and includes approximations for the maximum creep and shrinkage values from the refined methods.

$$\Delta f_{pLT} = 10 \frac{f_{pi} A_{ps}}{A_g} \gamma_h \gamma_{st} + 12 \gamma_h \gamma_{st} + \Delta f_{pR} \quad (2\text{-}15)$$

In which:

$\gamma_h = 1.7 + 0.01H$

$$\gamma_{st} = \frac{5}{(1 + f_{ci}^{'})}$$

Where:

f_{pi}= prestressing steel stress immediately prior to transfer (ksi)

H = the average annual ambient relative humidity (%)

γ_h= correction factor for relative humidity of the ambient air

γ_{st}= correction factor for specified concrete strength at time of prestress transfer to the concrete member

Δ_{fpR}= relaxation loss to be taken as 2.4 ksi for low relaxation strand.

1.8.2.2 Refined Estimates of Time-Dependent Losses

This method can provide a more accurate estimate for the total prestress losses when compared to the previously discussed method. This is because it calculates the losses from each time-dependent source, such as creep, shrinkage, and strand relaxation. This method can estimate losses during any stage of the construction process and for a wide range of the prestressed concrete girders with or without a topping slab. The time-dependent shrinkage loss is calculated in two steps, including the losses developed prior and after deck placement. The time can be adjusted to predict the loss at any time in the girder life.

The total losses are the sum of the losses due to creep, shrinkage, and relaxation from the time of transfer to the time of deck placement and from the time of deck placement to the final time as shown in the expression below. The gain in prestrsss due to shrinkage of bridge deck in composite section is not included.

$$\Delta f_{pLT} = \left[\Delta f_{pS} + \Delta f_{pC} + \Delta f_{pR}\right] id + \left[\Delta f_{pS} + \Delta f_{pC} + \Delta f_{pR} - \Delta f_{pSS}\right] df \qquad (2\text{-}16)$$

In which:

$(\Delta f_{pSR} + \Delta f_{pCR} + \Delta f_{pR1})id$: Refers to the losses from transfer to deck placement due to shrinkage, creep and relaxation, respectively.

$(\Delta f_{pSD} + \Delta f_{pCD} + \Delta f_{pR2} - \Delta f_{pSS})df$: Refers to the losses from deck placement to final time due to shrinkage, creep, and relaxation, respectively. The gain due to shrinkage of the composite deck concrete is subtracted from the total losses.

Δf_{pLT} = total losses in prestressing steel stress at final time

Δf_{pS} = losses due to shrinkage of girders concrete

Δf_{pC} =losses due to creep of girders concrete

Δf_{pR} = losses due to relaxation of prestressing force

Δf_{pSS} = gain in the girders prestressing force resulting from the shrinkage of the deck in the composite section at final time

Because this research is focused on prestress losses throughout construction, a brief description of prestress losses calculation is shown in the following sections. A detailed comparison of the prestress losses calculated using this method along with the measured values is presented in Chapter 5 of this report.

1.8.2.2.1 Losses at the Time of Deck Placement

Once the shrinkage strain is calculated according to eq. (2-27), the loss due to shrinkage of the girder concrete can be calculated using equation (2-17), per the 2014 AASHTO LRFD.

$$\Delta f_{pSR} = \varepsilon_{bid} E_p k_{id} \quad (2\text{-}17)$$

Where:

ε_{bid}= shrinkage strain girder concrete

E_p = modulus of elasticity of the prestressing strands

K_{id} = transformed section coefficient that accounts for time-dependent interaction between concrete and bonded steel and found as follows:

$$k_{df} = \frac{1}{1+\frac{E_p}{E_{ci}}\frac{A_{ps}}{A_g}\left[1+\frac{A_g e_{pc}^2}{I_g}\right]\left[1+0.7\psi_b(t_f,t_i)\right]} \quad (2\text{-}18)$$

In which:

e_{pg} = eccentricity of prestressing force measured from the girder centroid (in.)

$\Psi b(t_f, t_i)$ = creep coefficient at time of deck placement

t_i = age at transfer (days)

t_d = age at deck placement (days)

The prestressing force applied at transfer causes the concrete to creep, and this creep then decreases the prestressing force over time. The creep loss from transfer to deck placement is shown below in Eq. 2-19. This equation is equation (5.9.5.4.2b-1) in the AASHTO LRFD Bridge Design Specifications.

$$\Delta f_{pCR} = \frac{E_p}{E_{ci}} f_{cgp}\psi_b\left(t_d,t_i\right)K_{id} \quad (2\text{-}19)$$

Where:

E_{ci} = concrete modulus of elasticity at transfer

f_{cgp} = concrete stress at center of gravity of the prestressing strands

The equation below (2-20) gives the relaxation loss from the time of transfer to the time of deck placement.

$$\Delta f_{pR1} = \frac{f_{pt}}{K_L}\left[\frac{f_{pt}}{f_{py}} - 0.55\right] \quad (2\text{-}20)$$

Where:

Δf_{pR1} =prestress loss due to relaxation of prestressing strands between time of transfer and deck placement (ksi)

f_{pt} = stress in prestressing strands immediately after transfer, taken not less than 0.55f_{py} in Eq. 5.9.5.4.2c-1 of the 2014 AASHTO Code.

K_L = 30 for low relaxation strands and 7.0 for other prestressing steel, unless manufacturer's data are available.

1.8.2.2.2 Losses at the Final Time:

The final loss in the prestressing steel stress due to shrinkage is determined by multiplying the final shrinkage strain by the elastic modulus of the strands along with a reduction factor for the time-dependent interaction between concrete and bonded steel. The AASHTO LRFD Bridge Design Specifications provides equation (2-21) below to calculate the final shrinkage loss.

$$\Delta f_{pSD} = \varepsilon_{bdf} E_p K_{df} \qquad (2\text{-}21)$$

Where:

ε_{bdf} = concrete shrinkage strain taken between time of deck placement and final time

e_{pc} = eccentricity of prestressing force measured from the centroid of composite section (in.)

A_c = total area of the girder and the deck.

I_c = moment of inertia of the girder and deck composite section calculated using the deck-to girder modular ratio at service (in.^{4})

K_{df} = transformed section coefficient to account for time-dependent interaction between concrete and bonded steel and calculated as follows:

$\psi_b(t_f, t_i)$ = creep coefficient at time of deck placement

$$k_{df} = \frac{1}{1+\frac{E_p}{E_{ci}}\frac{A_{ps}}{A_c}\left[1+\frac{A_c e_{pc}^2}{I_c}\right]\left[1+0.7\psi_b(t_f,t_i)\right]} \qquad (2\text{-}22)$$

At the end of the structure's service life, prestress loss due to creep is calculated per equation (2-22) which is equation (5.9.5.4.3b-1) in the AASHTO LRFD Bridge Design Specifications.

$$\Delta f_{pCD} = \frac{E_p}{E_{ci}} f_{cgp}\left[\psi_b(t_f,t_i) - \psi_b(t_d,t_i)\right]k_{df} + \frac{E_p}{E_c}\Delta f_{cd}\psi_b(t_f,t_d)k_{df} \qquad (2\text{-}23)$$

Where:

Δ_{fcd} = long-term loss in the prestressing force due to creep combined with gain due to deck weight and superimposed loads (ksi)

$\Psi_b(t_f, t_d)$ = creep coefficient due to loading from deck placement to the final time

Long-term relaxation loss at final time is considered equal to the relaxation loss at deck placement:

$$\Delta f_{pR2} = \Delta f_{pR1} \qquad (2\text{-}24)$$

Shrinkage of the concrete deck in the composite section induces positive moment on the girder which increases the tension in the prestressing strands. This gain is calculated per the AASHTO LRFD Bridge Design Specifications as follows:

$$\Delta f_{pSS} = \frac{E_p}{E_c}\Delta f_{cdf} K_{df}\left[1 + 0.7\psi(t_f,t_d\right] \qquad (2\text{-}25)$$

Where:

Δf_{cdf} = change in concrete stress at the centroid of prestressing strands due to shrinkage of deck concrete (ksi) given as:

$$\Delta f_{cdf} = \frac{\varepsilon_{ddf} A_d E_{cd}}{\left[1 + 0.7\psi_d\left(t_f,t_d\right)\right]}\left[\frac{1}{A} - \frac{e_{pc}e_d}{I_c}\right] \qquad (2\text{-}26)$$

In which:

ε_{ddf} = shrinkage strain of deck concrete between placement and final time per Eq. (2-27)

A_d = dck area (in.^{2})

E_{cd} = modulus of elasticity of deck concrete (ksi)

e_d = eccentricity of deck measured from the centroid of the gross composite section (in.)

1.9 Prediction of Concrete Shrinkage

Shrinkage is the volumetric contraction of concrete over time without external load due to mainly the loss of the free water (Mehta and Monteiro 2006). In a prestressed concrete bridge girder, shrinkage reduces the girder length and strand elongation causing a loss in the prestressing force (Nilson, 1987). Shrinkage is affected by aggregate type, humidity, water-to-cement ratio, curing type, volume to surface area ratio of member, and duration of the drying period (AASHTO LRFD 2005).

1.9.1 AASHTO LRFD 2014

Shrinkage strain is calculated per AASHTO LRFD Bridge Design Specifications (Eq. 2-27) by applying correction factors to the maximum basic shrinkage strain. These factors include the effect of concrete strength, ambient humidity, volume-to-surface area ratio, and time as follows:

$$\varepsilon_{sh} = k_s k_{hs} k_f k_{td} 0.00048 \quad (2\text{-}27)$$

Where:

k_{hs} = shrinkage correction factor for ambient humidity

$= (2\text{-}0.14H)$ (2-28)

H = relative humidity (%).

k_s = factor for the effect of the volume-to-surface ratio of the component

$= 1.45 - 0.13(V/S) \geq 1.0$ (2-29)

k_f = factor for the effect of concrete strength $= \frac{5}{1+f_{ci}^{'}}$ (2-30)

k_{td} = time development factor $= \frac{t}{61-4f_{ci}^{'}+t}$ (2-31)

t = age of the concrete between end of curing and time to consider shrinkage effect, or between the time of loading and time to consider creep effect for creep calculations (days).

1.9.2 ACI 209R (1992)

The American Concrete Institute (ACI) provides the following equation to calculate shrinkage strain:

$$(\varepsilon_{sh})_t = \frac{t}{f+t}(\varepsilon_{sh})_u \gamma_{sh} \quad (2\text{-}32)$$

Where:

$(\varepsilon sh)_t$ = shrinkage strain at time t

$(\varepsilon sh)_u$ = ultimate shrinkage strain = 780×10^{-6} in/in

f = constant, 35 for the shrinkage after 7 days of moist cured concrete, and 55 for the shrinkage after 1-3 days for steam cured concrete

γ_{sh} = product of multiplying applicable correction factors to account for nonstandard conditions

1.10 Prediction of Concrete Creep Strain

Creep is the time-dependent deformation of concrete under a constant load. Creep strain depends on many factors such as the magnitude of loading, concrete maturity at loading, water to cement ratio, ambient humidity, and type and content of coarse aggregate (ACI Committee 209-92 2008). In prestressed concrete girders, the prestressing strands apply a compressive stress on the girder that shortens the girders and reduces strand elongation causing prestress losses over time. Creep coefficient, which is the ratio of the creep strain over the initial elastic strain, is used to account for the creep loss in the design of prestressed girders. The magnitude of creep coefficient depends primarily on the concrete strength at the time the prestressing force

is released or applied to the girder. The AASHTO LRFD Bridge Design Specification provides Eq. (5.4.2.3.2-1) to predict the creep coefficient. Some of the factors influence creep and shrinkage in the same way and were discussed in section 2.6.1. Two methods to predict the creep coefficient are presented in the following sections.

1.10.1 2014 AASHTO LRFD BRIDGE DESIGN SPECIFICATIONS

In the 2014 AASHTO LRFD Bridge Design Specifications, correction factors used for shrinkage strain are used to calculate the creep coefficient.

$$\psi(t,t_i) = 1.9 k_s k_{hc} k_f k_{td} t_i^{-0.118} \quad (2\text{-}33)$$

Where:

$\Psi(t,t_i)$: creep coefficient

k_{hc} = humidity factor for creep

$= 1.56 - 0.008H$ (2-34)

t_i = concrete age at loading (day)

1.10.2 ACI 209R-92 (2008) Method

The equation for the creep coefficient is given in the ACI 209R-92 Committee Report as:

$$v_t = \frac{t^{0.6}}{10 + t^{0.6}} v_u \quad (2\text{-}35)$$

Where:

v_t = creep coefficient at time t

v_u = ultimate creep coefficient = 2.35

γ_{sh} = product of multiplying applicable correction factors to account for nonstandard conditions and can be found as follows:

$\gamma_c = \gamma_{la} \cdot \gamma_\lambda \cdot \gamma_{vs} \cdot \gamma_s \cdot \gamma_\rho \cdot \gamma_\alpha$

1.11 Modulus of Elasticity of Concrete

The modulus of elasticity of concrete is the slope of the elastic portion of the stress strain curve under uniaxial compression stress. The elastic modulus of concrete depends on concrete compressive strength, unit weight, aggregate type and content, the use of mineral admixtures, and the properties of the interfacial transition zone (Mehta and Monteiro2013). Concrete is a nonhomogeneous material and its modulus of elasticity can vary. It is generally accepted that the modulus of elasticity is proportional to the square root of the concrete compressive strength. In addition, concrete with a higher unit weight also has a higher elastic modulus. Several models follow these trends when predicting the modulus of elasticity. However, studies show that accurate prediction of the modulus of elasticity requires including the effect of other factors, most importantly the coarse aggregate type (Al-Omaishi et al., 2009a), (Noguchi et al., 2009), (Aïtcin and Mehta1990) and the use of mineral admixtures (Noguchi et al., 2009). More discussion on the effect of coarse aggregate stiffness on the modulus of elasticity is presented in section 6.6 of this report.

Modulus of elasticity is an important parameter when predicting the camber and deflection of prestressed concrete girders. It is common practice in the design of prestressed concrete girders to take the modulus of elasticity measured at one-day of age and use this value to determine the camber at release. It also common practice to take the modulus of elasticity measured at measured at 28 or 56 days of age to determine the camber or deflection when the deck is placed and during service. Several studies indicate that modulus of elasticity at release affects the initial and the final camber significantly (Rosa et al., 2007).

1.11.1 Modulus of Elasticity Prediction Models

1.11.1.1 2010 AASHTO LRFD

The following equation estimates the modulus of elasticity for concrete with a unit weight between 0.090 and 0.155 kcf and a specified compressive strength up to 15.0 ksi:

$$E_c = 33000 k_1 W_c^{1.5} \sqrt{f_c'} \quad (2\text{-}36)$$

In which:

K_1 = correction factor to account for the course aggregate stiffness

w_c = unit weight of concrete (kcf)

f'_c = compressive strength of concrete at the time of consideration (ksi)

1.11.1.2 ACI 363R-92 (1992)

The ACI 363 committee recommends the following expression to predict the elastic modulus of normal density concrete with a compressive strength greater than 6.0 ksi (ACI Committee 363 1992). Neither concrete unit weight nor the stiffness of coarse aggregate is accounted for in this model as shown in Eq. (2-37). Several studies indicate that this equation underestimates the modulus of elasticity of high strength concrete (Tadros et al., 2003), (Al-Omaishi et al., 2009).

$$E_c = \left[1000 + 1265\sqrt{f_c'}\right]\left(\frac{W_c}{0.145}\right)^{1.5} \quad (2\text{-}37)$$

1.11.1.3 NCHRP Report 496 Method

The National Cooperative Highway Research Report Number 496 evaluated the effect of the coarse aggregate stiffness on the modulus of elasticity. The proposed formula is shown in Eq. (2-38). (Tadros et al., 2003).

$$E_c(t) = 33000 k_1 k_2 \left[0.14 + \frac{f_c'}{1000}\right]^{1.5} \sqrt{f_c'}\,(ksi) \quad (2\text{-}38)$$

1.11.1.4 ACI 318-08, AASHTO LRFD 2005

The AASHTOO 2005 and the ACI 318-08 recommend the expression in Eq. (2-39) to predict the modulus of elasticity of concrete.

$$E_c = 33000 \times W_c^{1.5} \sqrt{f_c'} \quad \text{(2-39)}$$

Concrete density is accounted for in this equation. This equation is applicable for concrete with a unit weight between 90 and 155 pcf. ACI 363 committee indicates that Eq. (2-39) overestimates the modulus of elasticity for concrete with compressive strengths over 6.0 ksi. That is also found by (Ahlborn et al., 2000).

CHAPTER THREE:

Field Measurements

2.1 Introduction:

At release, the tension force in the prestressing strands transfers to the concrete creating initial camber. This camber results from two main components. The first is the upward curvature caused by the eccentricity of the prestressing strands located in the bottom flanges, and the second is the member self-weight that deflects the girder downward. In a prestressed concrete girder, camber is influenced by several factors. The initial camber is influenced mainly by the modulus of elasticity of the concrete at release and the elastic shortening loss. However, the camber at the time of the girder erection is governed by time-dependent properties namely concrete creep, shrinkage, and strands relaxation. An accurate prediction of camber at any time requires an accurate prediction of all the influencing factors. It can be very challenging to estimate these properties during the design process of the prestressed concrete girder.

To evaluate various camber prediction models and to improve camber estimation methods used by the ARDOT, the research team conducted several visits to two precast concrete plants that produce prestressed bridge girders for the state of Arkansas. Extensive field data was collected for initial camber, camber growth, and concrete properties. In addition, strain gauges were used to monitor the change in the prestressing force and temperature gradient during production process. Details of the fabrication process and storage condition of the precast prestressed concrete girders were collected. This chapter includes details about the instrumented girders, measurements methods, and concrete materials tested in the field. The laboratory tests are presented in Chapter Four.

2.2 Girders Type and Details

ARDOT uses AAHTO-Type cross-sections for most precast-prestressed concrete girders. Currently, these girders are produced from precast prestressed concrete plants located in Tulsa, OK and Greenwood, MS. The experimental program included instrumenting and monitoring four types of girder which were AASHTO Type II, III, IV, and VI. For each type, the number of girders

investigated depended on the measurements that were conducted. For example, the release camber was measured for all the girders cast on the prestressing bed. This included three Type IV and six girders Type III girders. At later ages, camber was measured for additional girders. All girders were monitored for change in camber and strand strains at the time steps shown in Figure 3-1. The following sections cover details about the instrumented girders. Table 3-1 summarizes the main parameters for all girders.

Figure 3-1. Camber and strain monitoring times

2.2.1 AASHTO Type II Girder

The AASHTO Type II girders were 42 and 56 feet long and were used in two spans on the bridge. Each girder contained ten, ½-inch-diameter, grade 270, low-relaxation strands. As shown in Figure 3-2. Six strands continue straight along the bottom flanges, and four strands were in the top flanges and draped at two points. All Type II girders were manufactured at Coreslab Structures Inc. plant in Tulsa, OK and used in the widening of an existing bridge on Interstate I49 in Rogers, AR. At release, camber was measured for six girders placed at the same time and using the same concrete. Temperature and ambient humidity were recorded in conjunction with camber measurements. Figure 3-2 shows the cross sections at mid-span for Type II.

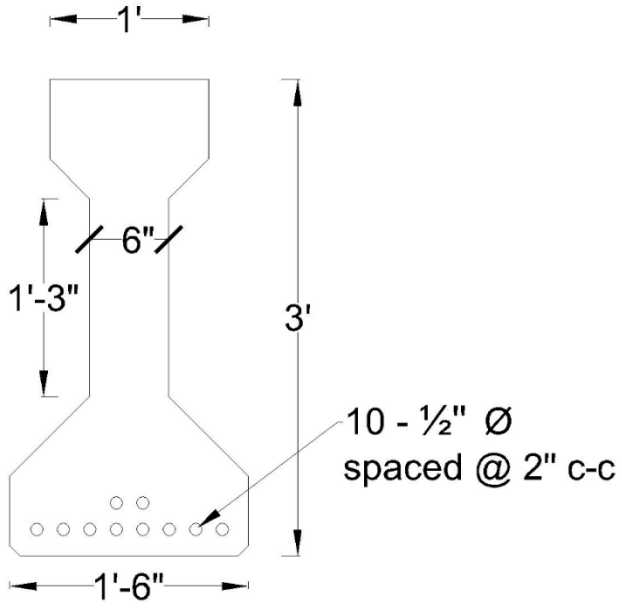

Figure 3-2. AASHTOO Type II cross section details at center

2.2.2 AASHTO Type III Girder

AASHTO Type III girders were manufactured at the Coreslab Structures Inc. plant and also used in widening of an existing bridge on Interstate I49 in Rogers, AR. These girders were 63 ft. long and contained 26, ½ -inch-diameter, grade 270, low-relaxation strands. The top flanges contained 4 straight strands and the bottom flanges contained 22 straight strands. Figure 3-3 shows the cross sectional details of the AASHTO Type III Girders.

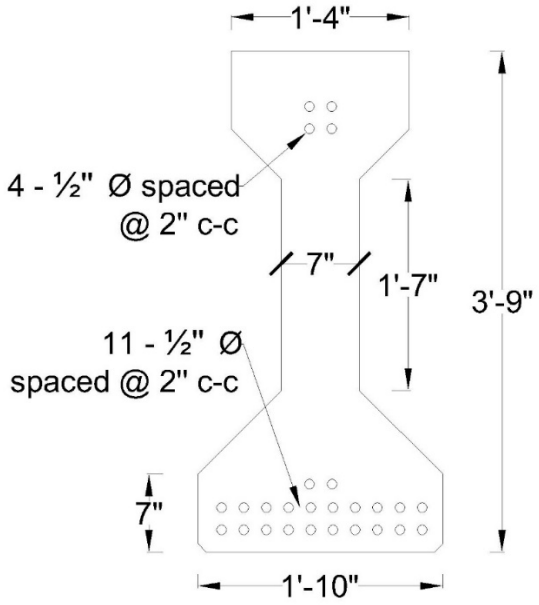

Figure 3-3. AASHTOO Type III cross section details at mid-span

2.2.3 AASHTO Type IV Girder

The AASHTO Type IV girders included in the study were 94 ft. long and manufactured at the J.J. Ferguson Prestress-Precast Co., Inc. plant in Greenwood, MS. These girders were used in construction of a bridge over the Ouachita River, 100 miles south of Little Rock, AR. Each girder contained 38, ½ inch-diameter, Grade 270, low-relaxation strands. All strands were straight with no harped points. Six strands were in the top flanges and the remaining were in the bottom flanges. Figure 3-4 shows cross section details of the AASHTO Type IV Girders.

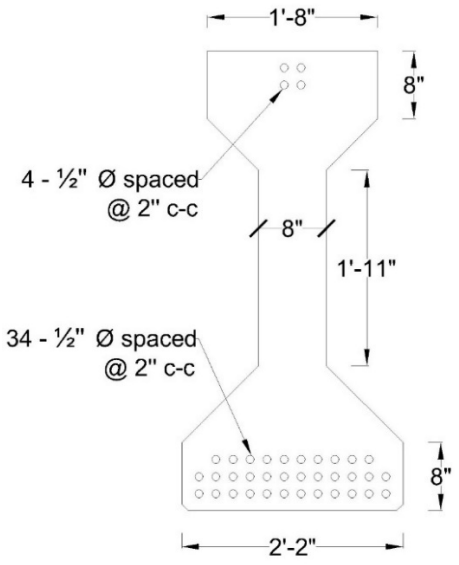

Figure 3-4. AASHTOO Type IV cross section details at mid-span

2.2.4 Type VI Girder

The experimental program also included instrumenting and monitoring cambers and strands stresses for AASHTO Type VI girders. The girders were 72 in. height and 109 ft. long. Type VI girders were manufactured in Tulsa, OK at the Coreslab Structures Inc. plant and used in construction of a new bridge located in Rogers, AR. Each girder contained 38 of 0.6 in. diameter low-relaxation strands. All strands were straight, and some strands were debonded at the ends. Figure 3-5 shows the cross section details for the AASHTO Type VI girders.

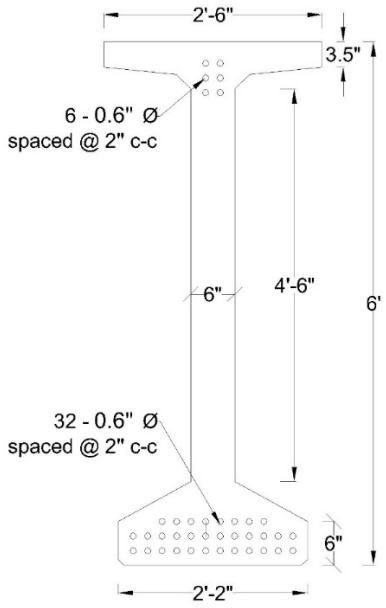

Figure 3-5. AASHTOO Type VI cross section details at center

Table 3-1. Summary of the girder details

Plant	Girders Type	Girder Length (ft)	Number of Strands	Strands Diameter	Strands Profile
Coreslab Structures	II	42 & 56	10	0.5	four strands harped
Coreslab Structures	III	63	26	0.5	straight
JJ Ferguson Prestress-Precast	IV	94	38	0.5	straight
Coreslab Structures	VI	109	38	0.6	straight

2.3 Camber Measurement

The camber was measured during all stages of the construction process in order to evaluate camber prediction methods and to develop a new prediction procedure that is presented in Chapter Five. As previously discussed, camber is affected by material properties, production practices, ambient temperature, relative humidity, and support conditions, (Storm et al., 2013), (Nguyen et al., 2015), (Tadros et al., 2011). Therefore, camber for a particular girder can vary

depending on the age and the time during the day. Given that, one should be cautious when monitoring camber growth for a group of girders, or when comparing the measured camber with the design values. For example, when exposed to direct sunlight, camber is generally higher than that measured on a cloudy day. Also, camber measured in the morning may differ from that measured in the afternoon (Nguyen et al., 2015). In this study, the research team was careful on performing all measurements for camber and strand strain at the same conditions as possible, especially for the girders belonging to the same type.

2.4 Camber Measurements Methods

In the beginning of the project, the research team tried different methods to measure the camber in order to find an accurate and practical method. These methods are discussed in the following sections. The procedure and limitations of each method is also discussed.

2.4.1 Automatic Level with Scaled Rod

The first camber measurements were made using an automatic level with a surveying rod. Reading were taken on the top surface of the top flanges at three locations along the girder. Two readings were taken at the ends and one at the girder mid-span. Because of the inconsistency of the top flange surfaces, the average of three reading was taken at each location. Camber was then calculated by averaging the end readings and subtracting that value from the midspan reading. Figure 3-6 shows the automatic level on top of the Type VI girders.

Figure 3-6. Automatic level positioned on top flanges surface to measure camber

The research team used this method during the first visit to Coreslab Structures Inc. in Tulsa, OK for measuring the camber of the 16 Type VI girders that had been in storage at the facility for over a year. As previously mentioned, there were inconsistencies in the surface of the top flange of the girders and this resulted in some variation in cambers when compared to other methods used to measure camber (which will be discussed later in this chapter). Figure 3-7 shows the differences between the cambers measured on the top flanges, and the camber of the same girders measured on the bottom flanges. This method also requires two people to take readings. This method may be best used when there is a limited number of girders. To eliminate the error associated with the inconsistent top flange surface, reading spots should be marked on the top flange before the strands are released. Reference readings, representing zero-camber before strand release, should be taken on the marked spots at the ends and the middle of the girders.

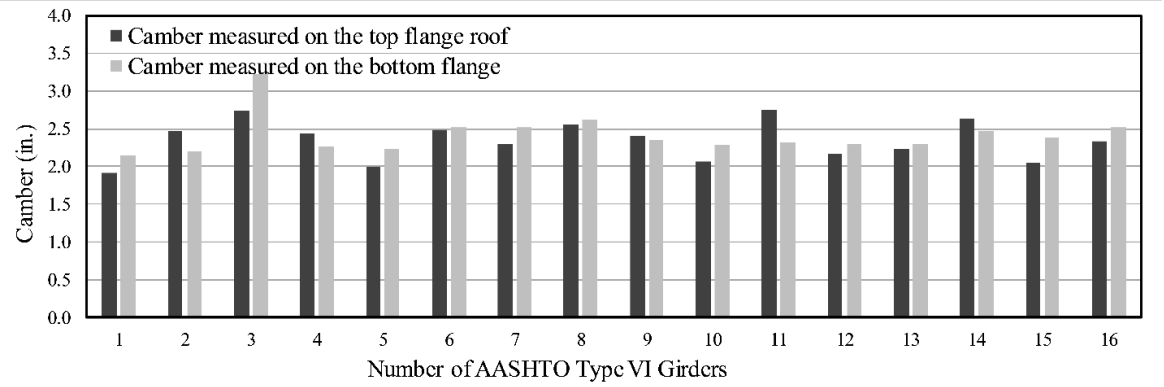

Figure 3-7. Comparison of cambers measurements taken on top and bottom flanges

2.4.2 Automatic Level with Wooden Template

The same automatic level was used to take readings on the top surface of the bottom flanges. As shown in Figure 3-8, a wooden template was manufactured to fit the section and be in contact with the web and the bottom flanges. Scales were attached on both sides of the template so that readings can be taken for two adjacent girders while keeping the level in the same station. For each girder, camber was calculated by averaging the readings at the end of the girders and subtracting it from the mid-span reading. This method works under the assumption that the bottom flange thickness is consistence. This method provides more accurate results when

compared to the previous one because readings were taken on smooth concrete unlike the surfaces of the top flanges.

Figure 3-8. Automatic level with wooden template used to measure camber of the bottom flanges.

2.4.3 Camber Measurements Using a Fishing Line

For some girders, a fishing wire was used to measure camber. As can be seen in the Figure (3-9, a) below, this method requires some simple tools to get a value for camber. However, it takes about 20 minutes to get the fishing line taut between the girder ends and touching the bottom surfaces of the top flanges. The fishing line was fixed at one end and allowed to move through a small groove made in a piece of wood in the other end of the girder. A weight was hung at the free end of the line to keep it tight. Camber was the vertical distance between the line and the bottom face of the top flange as shown in Figure (3-9, b)

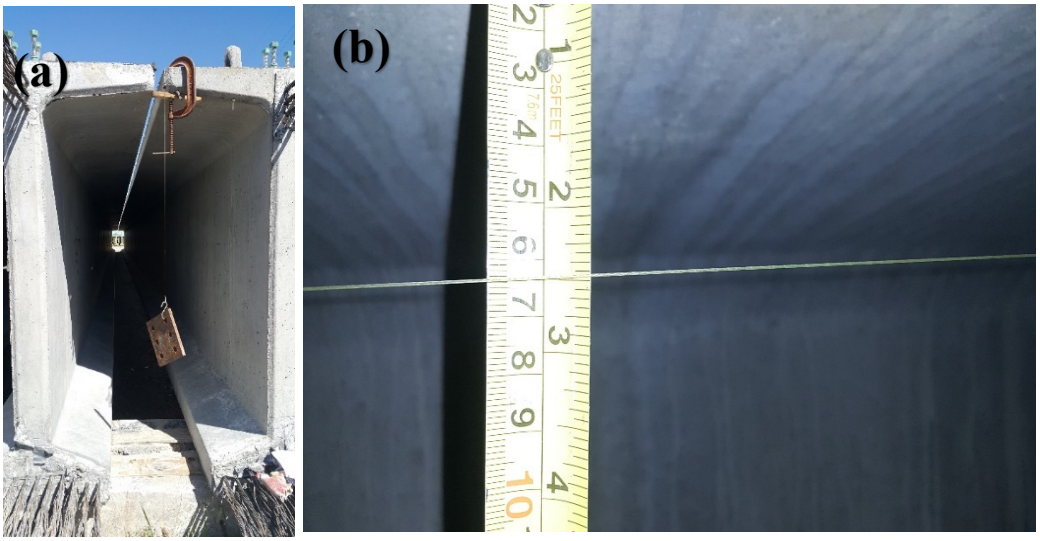

Figure 3-9. (a) Fishing line set up at the ends. (b) Camber measured at mid-span

2.4.4 Camber Measurements Using a Rotary Laser Level

As the project progressed, the research team decided to extend the type and the number of girders in the study to include AASHTO Type II and III along with Type VI. Also, one of the goals was to study the variability in camber of the same type of girder. Therefore, it was necessary to find an effective method of measuring camber that balanced accuracy with simplicity. The previous methods were time consuming and difficult to perform with long span girders. Also, it was necessary to decrease survey time to ensure consistency in the results by reducing changes in camber associated with increasing or decreasing temperatures.

A rotary laser level system proved to be more accurate and faster when compared to the previously used methods for measuring camber and deflection. The laser unit was stationed at the end of the girder, and three readings were taken along the girder span. The manufacturer-stated accuracy for the level used in the study was ±1/16 of an inch for each 100 ft. A laser detector was placed on a wooden rod with an aluminum scale on both sides to record the elevation. The rod had three contact locations that were kept in contact with the concrete when measuring elevations. Two points were in contact with the web to keep the rod vertical, and the third point ensured the rod was setting on the bottom flange. The rod was held perpendicular to the top flange surface using a level attached to the side. It was important to hold the rod in the

same manner when recording the elevations of the three points along the girder. The level and the rod are shown in Figure 3-10.

Figure 3-10. Rotary laser level and receiver rod used to measure camber

2.4.5 Tape Measure

For all girders, the initial camber was measured twice. Camber was first measured after prestress release when the girders were on the prestressing bed. Camber was measured again immediately after moving the girder to the storage yard. For determining the girder camber while on the prestressing bed, the mid-span of the girder was located. The distance at mid-span between the bed chamfer edge and the edge on the girder was measured using a tape measure. This distance was the initial camber. It is generally recognized that the friction between the girder ends and the steel bed restrain the camber from reaching its full potential. Therefore, the release camber did not reach its peak value immediately after release, instead it was measured before lifting the girder off the bed. This provided as much time as possible to obtain full transfer and the greatest camber. Figure (3-11) illustrates how the release camber was measured.

Figure 3-11. Release camber measurement

2.5 Materials Testing

One of the primarily reasons the actual camber deviates from the design value is that the engineers do not have an accurate estimation for the concrete material properties (O'Neill and French2012; Honarvar et al., 2015). Concrete properties such as compressive strength, elastic modulus, shrinkage, creep, and unit weight affect the prediction of camber and prestress losses (Stallings et al., 2003). Generally, the concrete material properties used during design may deviate from the actual concrete properties for several reasons. These reasons include differences in locally available materials and differences in the manufacturing/production practices. For example, some precast concrete facilities have developed and used a concrete mixture which achieves a compressive strength at release at the earliest possible time. This allows the manufacturer to increase the production process. Consequently, the concrete compressive strength at release and at later ages will be higher than the design strength. Concrete with a higher compressive strength will also have a higher elastic modulus which reduces the camber and prestress losses. Another example is coarse aggregate type. Concrete containing crushed limestone coarse aggregate has a different stiffness than concrete containing river gravel (Mehta and Monteiro 2013). Girder stiffness affects camber, self-weight deflection, and elastic shortening losses. More details on the effects of coarse aggregate stiffness on concrete properties are presented in Chapter Six.

In this study, the researchers were present during the manufacture of all girders and sampled concrete specimens from all mixtures used to cast the girders. Fresh and hardened concrete were conducted using the plant laboratory equipment. At later ages, tests were conducted at the Engineering Research Center at the University of Arkansas. The following sections describe the tests, samples collected, and production details.

2.6 Preparing the Concrete Testing Specimens

Material tests were performed on the concrete used to cast the 21 girders. The 21 girders consisted of three AASHTO Type IV girders and six for each AASHTO Type II, III, and VI girders. For each girder type, the research team chose one or two castings to collect a sample of concrete to cast specimens for material property tests.

More than 30 cylinders and 6 prisms were prepared from the concrete used to cast each type of the AASHTO girders. The concrete cylinders were 4 × 8 in., and the shrinkage test prisms were 4 × 4 × 11¼ in. Concrete was collected from each girder on the prestressing bed when possible and from at least three different mixers. This was done in order to make the specimens more representative of the concrete, which comprised each girder. The specimens were placed beside the girders under the tarps to mimic the curing conditions of the girders. Before opening the forms, the concrete cylinders and the prisms were collected and kept in the molds until the test day. Figure 3-12 shows the specimens beside the girders during the curing period.

The compressive strength, modulus of elasticity, shrinkage, and creep were measured for all mixture proportions. Test results and a comparison with the design values are discussed in Chapter Six. Whenever concrete was sampled, the researchers stayed at the plant to measure the release camber and the initial prestress losses.

Figure 3-12. Concrete specimens stored under the tarps during curing the girders

2.7 Compressive Strength and Modulus of Elasticity Testing

At the Coreslab Structures Inc. plant in Tulsa, OK, the curing time for the Type II, III, and VI girders was approximately 16 hours. At midnight, after about 14 hours from casting, the laboratory technician tested one cylinder that was stored under the tarps. If the specified design strength was not achieved, the technician would wait an additional hour and test a second cylinder. Once the release strength was achieved, two more cylinders were tested to record the average compressive strength of three cylinders. The researchers used the data obtained by the facility for compressive strength at release and at 28-days for the Type II, III, and VI girders.

It is important to point out that the release of the prestressing force occurs four to five hours after compressive strength test. Therefore, the actual compressive strength at release is higher than that tested by the plant laboratory technician. This time is required for removing the tarps and opening the form sides. Also, the plant staff are not authorized to open the forms until the release strength meets the design value. Therefore, the research team tested the compressive strength and the modulus of elasticity at the same time of strand release. The difference in compressive strength between when the cylinders were first tested and when the strands release ranged from 7% to 14 % (higher). The modulus of elasticity was measured at the same time the strands were released which also corresponded to the time the compressive strength was measured. An end grinder (for preparing the ends of the cylinder for the elastic modulus test) was not available at either plant, so unbounded caps were used in both tests (compressive

strength and elastic modulus). The concrete cylinders were demolded at the same time the girders were removed from their forms.

At the J.J. Ferguson Prestress-Precast Co., Inc. facility, the strands were detensioned between 20 to 24 hours after casting. The girders were cast at approximately 8:00 AM, and the compressive strength was tested at approximately 7:00 AM of the next day. As with the Coreslab Structures Inc. facility, there was also a time difference between the time the compressive strength tests were performed by the laboratory technician and the actual release time. The compressive strength and elastic modulus results shown in this report were performed by the researcher approximately 30 minutes after strand release.

2.8 Girders Curing Procedure

The curing regimens for the girders differed between the plants and within an individual plant. The curing regimens were based on plant strategy and the ambient temperature. Steam curing was sometimes used to expedite the production process. In this study, the girders were cast in different seasons and therefore subjected to different curing regimes. Table 3-2 lists the curing regimens used for each girder type. For the Type VI girders that were cast in August 2016, the curing was neither steam nor moist cured. Instead, it was combination of both. After casting, the girders were covered with an insulated, layered tarp that preserved the heat generated from the cement hydration until the time of release. Also, there were small hoses that provided a constant source of moisture continuously to keep the top flanges wet. The heat generated from cement hydration exceeded 55 C^o which was enough for the concrete to gain the release strength in less than 16 hours.

Table 3-2. Curing type and casting date for the girders

Plant	Girder Type	Date Cast	Curing Type	Ave. Concrete Temperature at release (C^o)
Coreslab Structure	II	12/22/2016	Steam	43
Coreslab Structure	III	1/11/2017	Steam	52
J J Ferguson Prestress-Precast	IV	2/10/2017	Steam	47

Coreslab Structure	VI	9/15/2016	Water	53

2.9 Strands Strain Measurements

Camber in prestressed girders is created by the eccentricity of the prestressing force. Therefore, any attempt to quantify camber behavior would not be successful without field assessment of the strand stress. In this study, field measurements for camber, deflection and concrete properties were made in conjunction with measurements for the strand strain over time. Measuring the strain of the prestressing strands will not only improve camber prediction but will also help assessing the accuracy of the prestress loss prediction methods.

Vibrating wire strain gages were embedded in nine prestressed concrete bridge girders used in three bridges within the state of Arkansas. The strain gages were placed after tensioning the strands and before installing the formwork. One strain gauge was attached to the bottom strands and a second gage was attached to the top stands or in the center of the top flanges when the strands were harped to the bottom flanges. These gages provided temperature readings as well. Concrete temperature was essential to measure the hydration temperature, thermal gradient along the girders' height, and to correct the strain reading due to the differences in the thermal expansion coefficient between the strands and the concrete. Figure 3-13 shows the strain gages attached to the prestressing strands before placing the concrete.

Figure 3-13. Strain gages attached to the prestressing strands

Two girders were instrumented for each girder type, except for the AASHTO Type VI girders, for which, three girders were instrumented. Strand strain and concrete temperature were recorded several times before and after placing the concrete. However, the zero reading for prestress losses measurement was taken just before release. A manual, handheld data reading device was used to record the strain. The strain was then multiplied by the modulus of elasticity of the strand to determine strand stress. Comparisons of the measured and calculated prestress losses are discussed in Chapter Five of this report.

CHAPTER FOUR:

Laboratory Measurements

3.1 Introduction

Camber at girder erection, which is of interest to designers and contractors, is influenced by concrete creep and shrinkage. After release, the prestress force decreases with time due to the shortening of the girder's length resulting from both creep and shrinkage. This reduction in the prestressing force affects camber. To predict camber at any time after release, an accurate estimate for the creep and shrinkage strain is necessary. Therefore, extensive laboratory tests were conducted in conjunction with the field measurements to improve the prediction of time-dependent concrete deformation and the elastic modulus of concrete. In this project, creep and shrinkage were measured from the concrete sampled during the casting of the girders. Additionally, specimens were prepared at the lab using the same mix proportion used in the girders. This chapter presents a detailed description of the laboratory tests for creep, shrinkage, and modulus of elasticity.

3.2 Shrinkage Test

Laboratory tests were performed to determine the shrinkage strain of the concrete mixtures used in the girders. Concrete prisms were cast for each girder type. During the casting of the girders, six concrete prisms were cast and cured beside the girders under the tarps. The prisms were 4 in. × 4 in. × 11¼ in. After approximately 24 hours, the prisms were shipped to the engineering research center at University of Arkansas and demolded. Once demolded, the initial comparator readings were recorded. It should be noted that two curing procedures were followed in the shrinkage test. The first procedure followed the ASTM C157/C157M "Standard Test Method for Length Change of Hardened Hydraulic-Cement Mortar and Concrete". For this curing regimen, three prisms were cured in lime-saturated water at 73 ± 3 °F for 28 days. After the 28 days of curing, the prisms were removed from the water storage, wiped with a damp cloth and measured for the second comparator readings. Readings for each prism were taken at 4, 7, 14, and 28 days and then monthly for approximately one year.

The second curing procedure did not follow the ASTM method. These prisms were not submerged in water because this more closely represented the actual conditions of the girders. After an initial reading, the specimens were stored at a temperature of 73 ± 3 °F. The comparator readings were also taken at 4, 7, 14, 28 days and then once monthly for approximately a year. Shrinkage strain was calculated by dividing the change in the prism length by the gauge length as shown in Eq. (4-1) below. Figure 4-1 shows the shrinkage strain measuring device. Shrinkage strain test results for each type of girder and a comparison with the prediction model are presented in section 6.4.

$$\varepsilon_t = \frac{L_t - L_{initial}}{10} \tag{4-1}$$

Where:

L_t= prism length reading at time t

$L_{initial}$= initial prism length reading after at time t

Gage length = 10 in.

Figure 4-1. Shrinkage strain measurement

3.3 Creep Test

Concrete creep affects the behavior of prestressed concrete girders. Concrete creep causes a loss in the prestressing force and increases camber over time. The effect of concrete creep strain is accounted for in the design calculations through the creep coefficient. The creep coefficient is the ratio of the creep strain to the elastic strain. Creep strain is influenced by the hardened concrete properties, mixture proportion, and type of coarse aggregate. Therefore, accurate prediction of creep requires laboratory testing on concrete specimens prepared with the same concrete materials and properties.

Creep tests were performed on concrete cylinders made with the same mixture proportion and materials used to cast the girders. Creep tests were conducted using eight concrete cylinders with dimension of 4 in. × 8 in. The cylinder ends were ground and checked for planeness and uniform diameters. Two cylinders were tested in compression, two were kept unloaded to measure the shrinkage strain, and the remaining four cylinders were loaded in the creep frame. Two of the loaded cylinders were sealed with an epoxy to prevent the effect of moisture movement from and into the concrete cylinders.

3.3.1 Creep Test Frame

Frames were assembled to apply a constant load on four concrete cylinders. As shown in Figure 4-2, a hydraulic jack was used to compress four steel springs in the bottom of the frame. The springs are used to create a sustained load on the concrete cylinders after the hydraulic jack was removed. The springs were Type D2 Outer with a stiffness coefficient of 9,821 lb./in. The four springs can be compressed 1.5 in. which is enough to apply a force of 58,926 lb. on the cylinders. This allows the research team to conduct the creep tests on concrete with a compressive strength up to 12 ksi for 4×8 in. cylinders based on ASTM C512.

It should be noted that using steel balls between the steel plates and the top and bottom of the concrete cylinders was not useful in distributing the load over the cylinders cross section as recommended in the ASTM C512. In the first test, the steel balls caused a rotation in the top and the bottom plates that could buckle the cylinders during loading. After several trials and

adjustments to the eccentricity in the frame, the balls created large punching stress in the plate's center and showed a tendency to slip causing a safety concern.

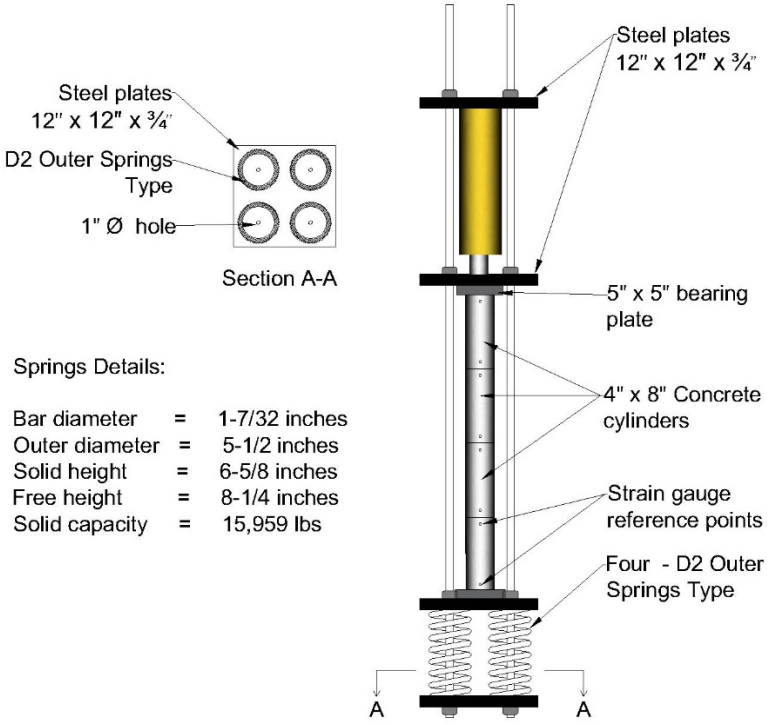

Figure 4-2. Frame details for the creep test

3.3.2 Loading

Before loading, two cylinders were tested to determine the compressive strength. Also, before loading, the initial zero readings were taken on each side of all cylinders. An initial load of 5000 lb. was applied to examine the cylinders' eccentricity by comparing the strain on the four sides of the top and bottom cylinders. The controlling nuts shown in Figure 4-2 were used to balance the strain between the four sides of the concrete cylinders. A hydraulic pump applied the load by compressing the bottom springs. The pump was equipped with a hydraulic pressure sensor which was connected to a computer. The load and the compressed length for the cylinders were recorded.

3.3.3 Strain Measurements

Reference discs were glued onto the four sides of the cylinders before applying any load (Figure 4-3a). The gauge points were distributed over the cylinders and at least two vertical measurements were taken for each side of the concrete cylinders. Creep strains were obtained using the Mechanical Strain Gauge shown in Figure 4-4. Figure 4-3 (b). shows the loaded creep frames during testing.

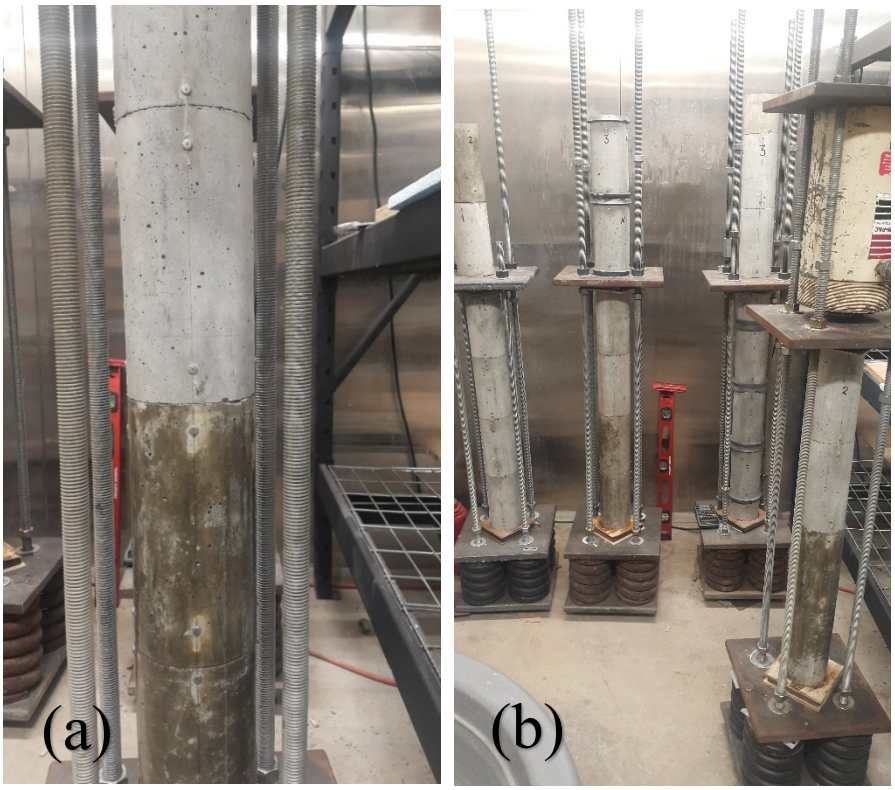

Figure 4-3 (a) DEMEC points attached to the concrete cylinders. (b) Loaded creep frames.

To obtain accurate strain measurements during the creep test, the gauge length must be less than the concrete cylinder length. This ensures that the reference discs are attached to one individual cylinder. If the joint between the ends of two cylinders was included in the strain measurements, the elastic strain in the joint would provide a false measurement. In this project, a multi length, mechanical strain gauge was used to measure the length change between the reference discs (Figure 4-4). The gauge length was six inches. The mechanical strain gauge had a precision of 0.0001 in. Readings were repeated at least three times. As specified in ASTM C512,

measurements were taken daily for the first week, weekly for the first month, and at larger intervals later. The creep strain results will be discussed in Section 6.5.

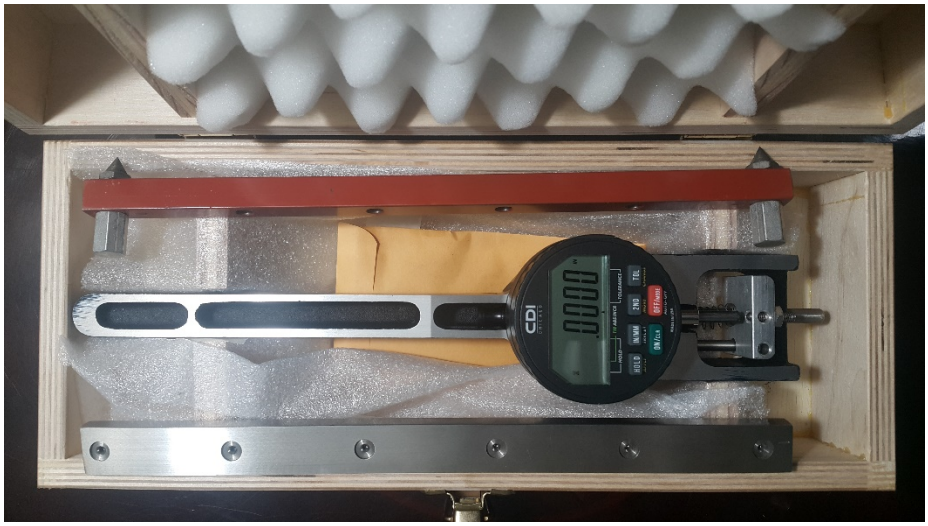

Figure 4-4. DEMEC gage device used in creep strain measurements

3.4 Determining the K_1 Coefficient for the Coarse Aggregate

This project also focused on determining the stiffness coefficient, K_1, for three types of coarse aggregate typically used in girders for Arkansas bridges. Because different types of coarse aggregates produce concrete with different modulus of elasticity, the K_1 coefficient accounts for the effect of coarse aggregate stiffness in the prediction of the concrete's elastic modulus. Focus was placed on improving the prediction of the modulus of elasticity because it is required in calculating camber, deflection, and prestress losses. The following sections cover details about the coarse aggregate types and gradation and concrete mixtures used in preparing the modulus of elasticity test specimens.

3.4.1 Coarse Aggregate Types and Gradation

The coarse aggregates were sampled from three different quarries. The crushed limestone was from Benton County Stone quarry in Sulphur Springs, AR. This quarry produces the coarse aggregate used in girders produced at the Coreslab Structures Inc. plant in Tulsa, OK. This plant fabricated the AASHTO Type II, III, and VI girders. The J.J. Ferguson Prestress-Precast Co., Inc. plant which fabricated the AASHTO Type IV girders used river gravel. The research team obtained the gravel from the same source that provided the aggregate for the plant in Greenwood, MS. The third type of coarse aggregate was a crushed limestone from a quarry in Springdale, AR. This aggregate is commonly used in Northwest Arkansas. Table 4-1 shows the gradation for the three types of aggregate.

Table 4-1. Gradation for the three types of coarse aggregate.

Sieve Size	Seive Size (in.)	% Passing			Standard Gradation ARDOT Spec.	Alternative Gradation AASHTO M43 #57 Spec.
		Crushed Limestone (Springdale, AR)	River Gravel (Greenwood, MS)	Crushed Limestone (Sulphur Springs, AR)		
2 in.	2.500	100	100	100	-	-
1 1/2 in.	2.000	100	100	100	-	100
1 1/4 in.	1.500	100	100	100	100	-
1 in.	1.000	100	100	100	60-100	95-100
3/4 in.	0.750	95	94	98	35 - 75	-
1/2 in.	0.500	59	52	61	-	25-60
3/8 in.	0.375	43	32	38	10 - 30	-
No. 4	0.187	7	8	3	0 - 5	0 - 10
No. 8	0.093	1.0	5.3	0.7	-	0 - 5
No. 16	0.047	0.7	5.3	0.5	-	-
No. 30	0.024	0.6	5.3	0.5	-	-
No. 50	0.012	0.4	5.3	0.5	-	-
No. 100	0.006	0	5	0	-	-
No. 200	0.003	0	5	0	-	-
Pan	0.000	0	5	0	-	-

Aggregate porosity, content, size, shape, and surface texture affects the strength and stiffness of concrete. For example, a denser coarse aggregate may lead to concrete with higher

strain capacity (Mehta and Monteiro 2013). A single equation may not provide reliable estimates for the elastic modules of concrete mixed with any type of aggregate. Accurate prediction of the elastic modulus requires accounting for the effect of coarse aggregate stiffness through extensive laboratory testing for the compressive strength, unit weight and elastic modulus.

3.4.2 Concrete Mixtures and Testing

From each type of aggregate, several concrete mixtures were made with a target compressive strength ranging from 5.0 to 11.0 ksi. Unit weight, slump and, for some mixtures, the air content were the fresh concrete properties measured. The mixtures were not air entrained and therefore the only air in the concrete was entrapped air. This is why the air content was not measured for all mixtures. Compressive strength and modulus of elasticity was measured at 1, 7, 28, and 56 days on 4 in. × 8 in. cylinders. At each age, typically three cylinders were tested for compressive strength, and then three cylinders were tested for elastic modulus. Compressive strength and modulus of elasticity were tested according to the ASTM C39 and ASTM C469, respectively. **Table 4-2** shows mixtures proportion used for preparing the test specimens.

Table 4-2. Concrete mixtures used for the modulus of elasticity testing specimens.

Material	**Mix 1**	**Mix 2**	**Mix 3**	**Mix 4**	**Mix 5**	**Mix 6**	**Mix 7**	**Mix 8**
Cement (lb/yd^3)	520	550	564	600	611	658	668	705
Coarse aggregate (lb/yd^3)	1700	1640	1760	1700	1835	1924	1900	1900
Fine aggregate (lb/yd^3)	1456	1517	1541	1485	1417	1271	1237	1161
Water (lb/yd^3)	276	264	234	270	238	230	234	282
Measured Properties								
Air %	-	-	3.1	1.7	1.5	-	-	1.8
Water / Cement ratio	0.53	0.48	0.415	0.45	0.39	0.35	0.35	0.4
High range water reducer (fl oz/cwt)	2	7	5.5	8	8.5	6	8	7
Slump (in.)	4.0	6.5	2.75	7.0	7.0	7.0	6.5	10.0
Average 28-day Compressive Strength (psi)	5530	7440	8300	9680	10000	10510	11560	9830

CHAPTER FIVE

Comparison of Calculated and Measured Cambers, Deflection, and Prestress Losses

4.1 Camber Measurements

As previously discussed, improving camber estimates during all phases of construction can reduce construction and maintenance costs. In this study, camber was measured for several girders from strand release to deck placement. The research team conducted several trips to the two precast plants and bridge sites to measure the girders cambers or deflections. A rotary laser level was used for most measurements. The initial camber was measured immediately after cutting the strands. Camber at girder erection was measured at the bridge site before the deck reinforcement was placed.

4.2 Measured Versus Design Erection Camber

At the time of this report, the AASHTO Type IV girders have not been erected at the bridge site due to a construction delay related to seasonal flooding. However, the erection camber is assumed to be the measured camber for the girders stored in the precaster's yard for more than three months. Several studies assumed 120 days as the age of the girders at the time of erection (Tadros et al., 2011).

Field measurements revealed differences between the predicted and the measured camber for all girders. Figures (5-1) through (5-4) compare the measured camber with the design values using different methods for each type of girder. The predicted (or design) camber at erection is greater than the averaged measured camber by 93%, 128%, 72%, and 25% for the AASHTO Type II, III, IV, VI girders, respectively. Using the PCI Multiplier Method with the transformed section properties resulted in better camber prediction when compared to the same method with the gross section properties. In general, the differences between the design and the measured camber are higher in short girders (Type II and III) than in long girders (Type IV and VI). The main reason why the erection camber was less than the design value was due to the concrete compressive strength being higher than the design strength. This conclusion was also determined by other researchers (O'Neill and French 2012). Higher concrete compressive strength increases

girder stiffness which reduces the camber at the time of release. The measured compressive strength for all girders is discussed in greater detail in Chapter 6, section 6.1. Another reason for the over estimation of camber can be attributed to the current design method used by ARDOT as discussed in section 5.3.

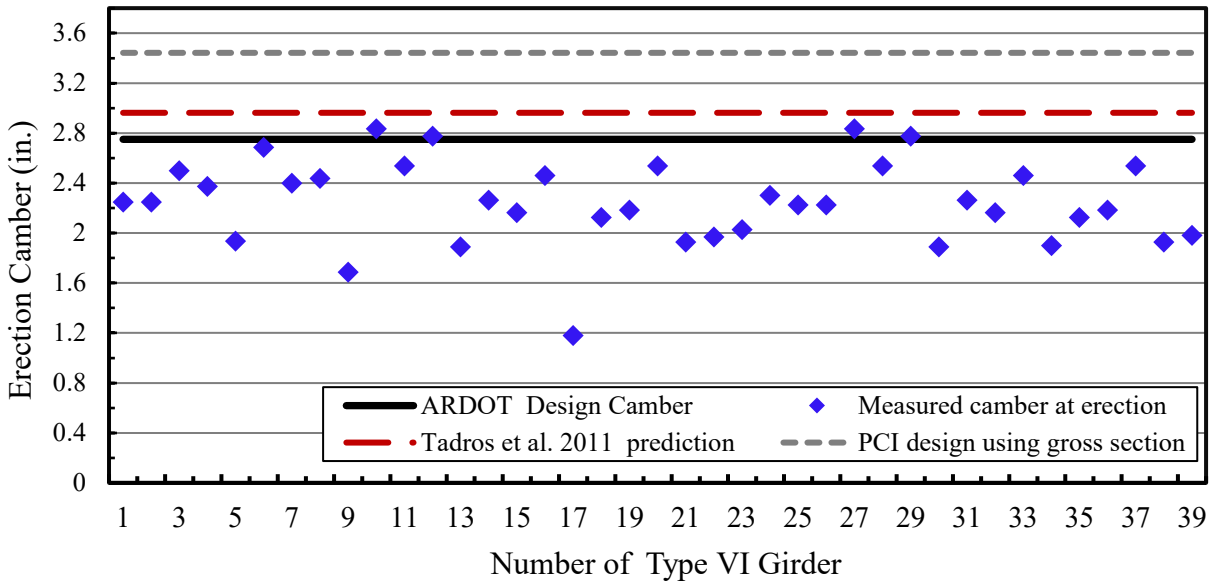

Figure 5-1 Comparison between the design and the measured erection camber for AASHTO Type VI girders

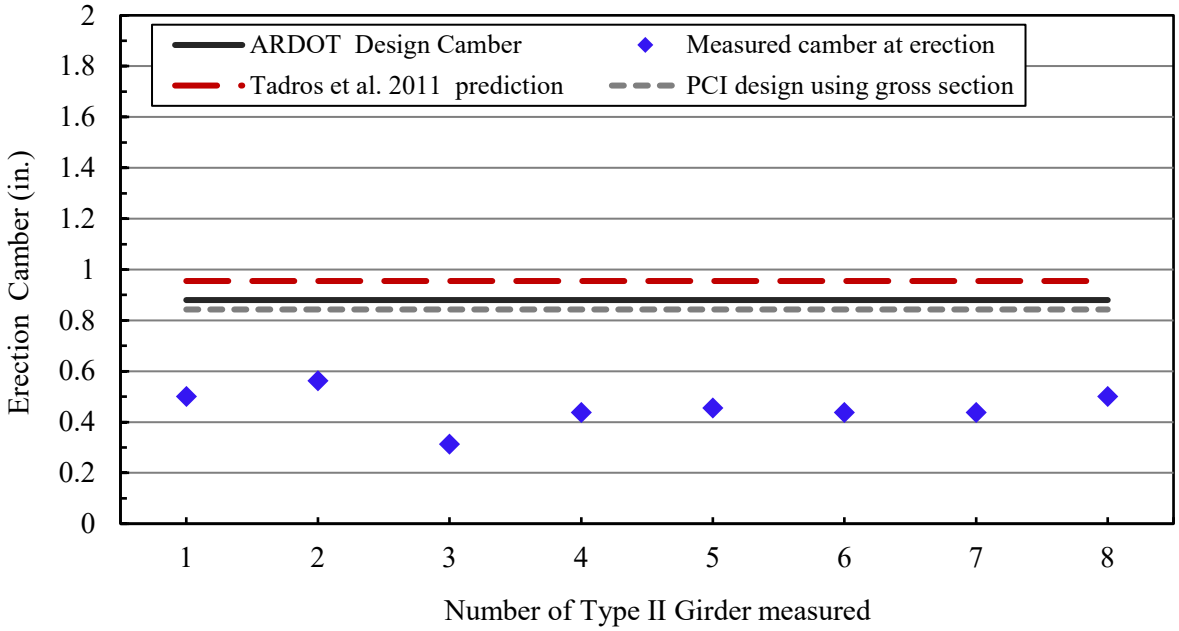

Figure 5-2 Comparison between the design and the measured erection camber for AASHTO Type II girders

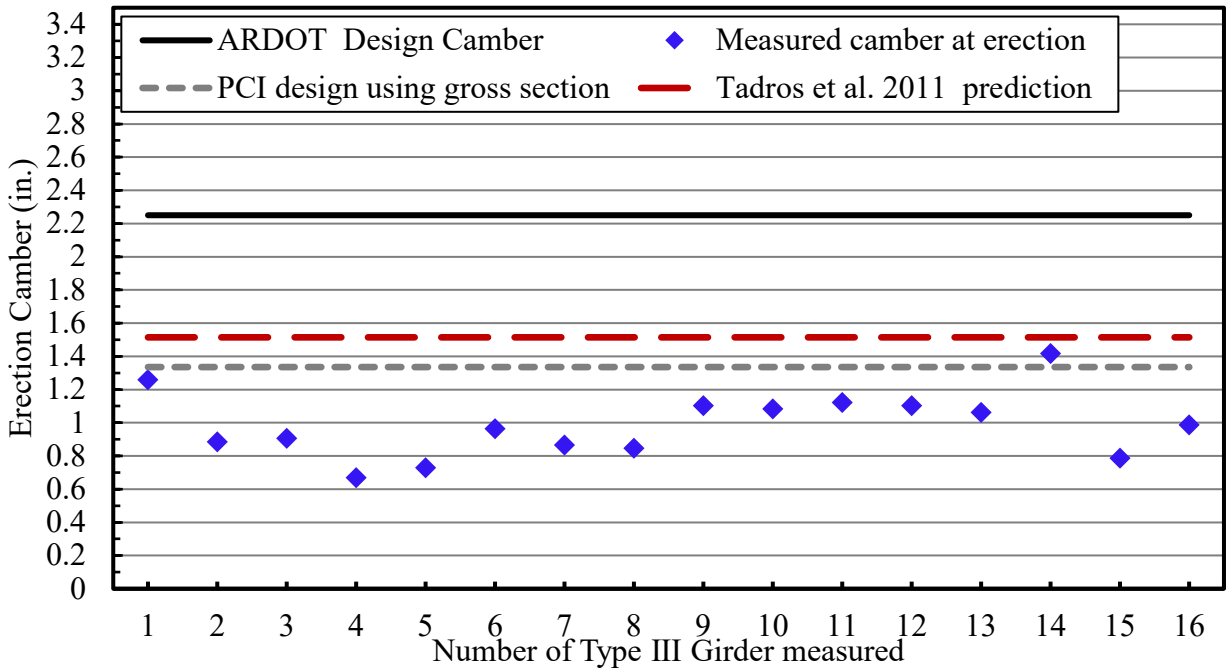

Figure 5-3 Comparison between the design and the measured erection camber for AASHTO Type III girders

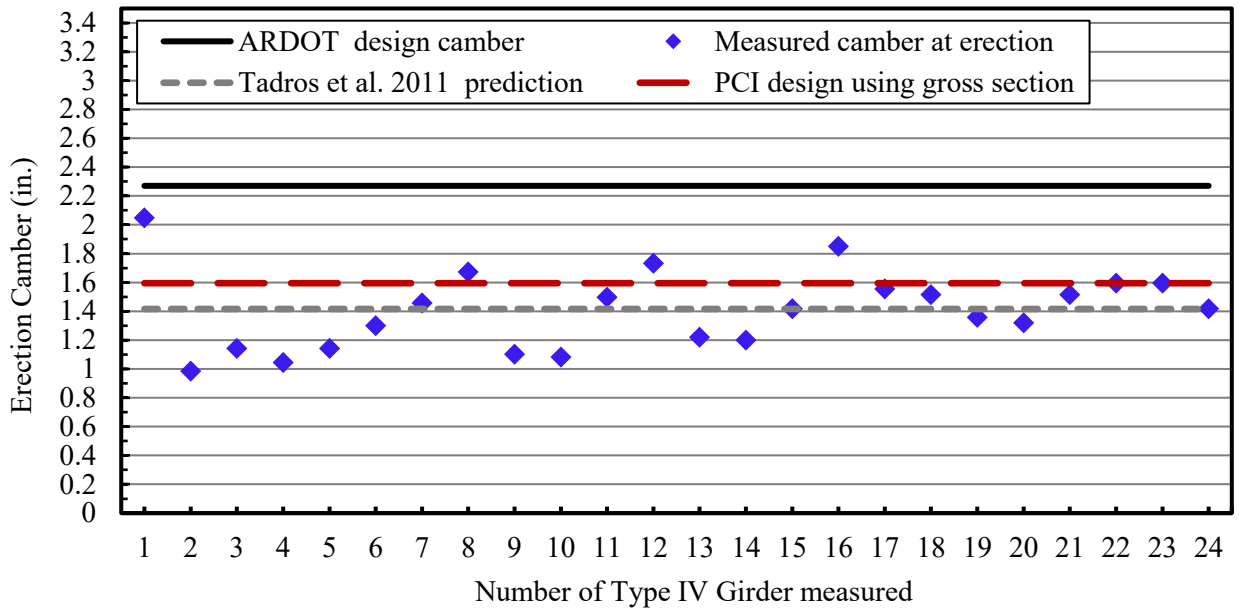

Figure 5-4. Comparison between the design and the measured erection camber for AASHTO Type IV girders.

4.3 Evaluation of Camber Prediction Method

Materials testing and field measurements were used to examine the accuracy of the PCI Multiplier Method and the ARDOT method (PCI 2010). Figure 5-5 compares the measured camber at erection with the predicted (or design) values calculated with the PCI and ARDOT methods. When using the actual concrete properties along with the measured elastic shortening loss, the PCI multiplier method provided a reasonable estimate for the erection camber. ***The difference between the design and the measured erection camber did not exceed 0.5 in.*** Although these differences may be acceptable, unless there are historical values for the concrete properties and strand stress from the precast plant, the actual concrete properties and the initial prestress losses are not available at the design stage. However, this report will provide the designers with guidelines to accurately estimate concrete properties and strand stress needed for camber design.

As previously mentioned, the ARDOT camber prediction procedure over-estimates camber at erection. The construction plans provide the erection camber at 90 days from release. This camber is calculated using the specified concrete compressive strength and the estimated strand stress. However, even when using the same parameters (specified concrete strength and estimated strand stress), the PCI multiplier method provides a better estimate for camber. As illustrated in Figure 5-5, the ARDOT method results in the highest estimated camber for all girders. The ARDOT design method results in camber higher than the measured by 93%, 128%, 61%, and 25% for AASHTO Type II, III, IV, VI girders respectively. Based on these results, changes could be made to the ARDOT camber prediction method.

As can be seen from Figure 5-5, the differences between predicted and measured camber is larger in the short girders, Type II and III girders. The reason for that is the differences between the design and the actual (used) concrete compressive strength is greater in short girders. While short girders may require a lower concrete strength than girders with longer spans, the common practice in both precasting plants is to use one concrete mixture for multiple projects even when the concrete strength is much higher than the required. For example, a few AASHTO Type II and III girders were needed for widening an existing bridge on the I49 in Rogers, AR. Therefore, the fabricators at Coreslab Structures Inc. facility preferred to use the same concrete mixture

proportion used in the AASHTO Type VI girders. This was done to avoid the risk of affecting concrete properties such as the air content, slump, and the compressive strength when changing to a different mixture proportion. An over designed concrete mixture achieves the design release strength at an earlier time which then shortens the production cycle.

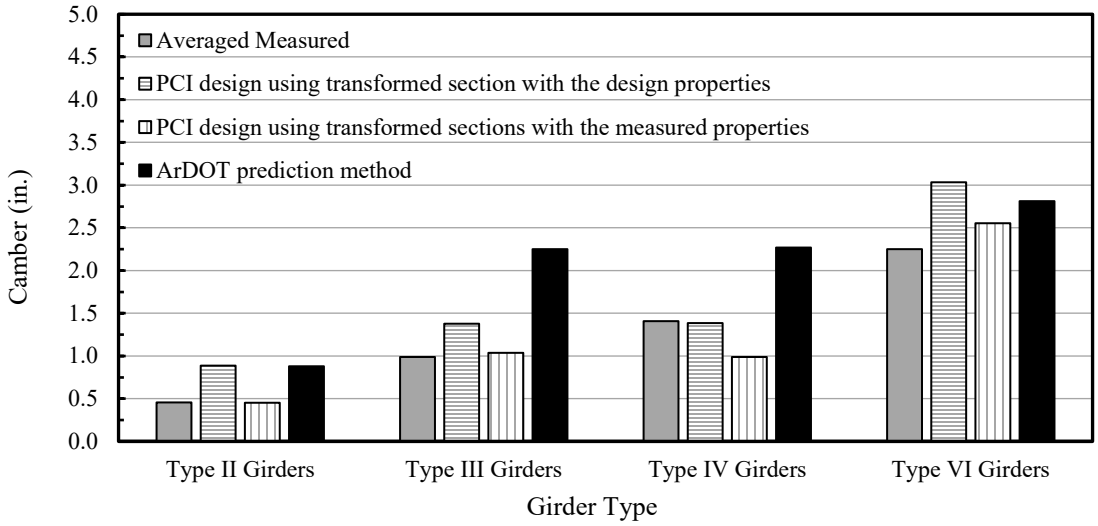

Figure 5-5. Comparison of the averaged measured camber at erection with the predicted values.

4.4 Recommended Camber Prediction

Based on the observations from the material tests and the field measurements, a modification to the PCI multipliers method was recommended to predict camber at girders erection. The PCI design method utilizes two multipliers: 1.85 for the initial elastic deflection from the member weight and 1.8 for the initial elastic camber from the prestressing force at release as shown in Eq. (5-1) (PCI 2010). The recommended method utilizes a single multiplier of 1.4 times the elastic camber (initial camber at release) calculated using gross section properties as shown in Eq. (5-2). This multiplier was validated using the camber measurements conducted at girder erection. Figures (5-6) through (5-9) compare the measured camber to the design camber using the recommended multiplier. This multiplier is applied to the design initial camber and improves the prediction. The estimated error ranges from -8% to 18% which is less than 0.5 in.

when compared to the actual camber. This error can be easily adjusted using the haunches. The proposed 1.4 factor is conservative way to ensure the required deck thickness is maintained.

$$\Delta_{\text{erection camber}} = 1.8\ (\uparrow \Delta_{\text{prestress}}) - 1.85\ (\downarrow \Delta_{\text{self-weight}}) \quad (5\text{-}1)$$

$$\Delta_{\text{erection camber}} = 1.4 \times (\uparrow \Delta_{\text{initial}}) \quad (5\text{-}2)$$

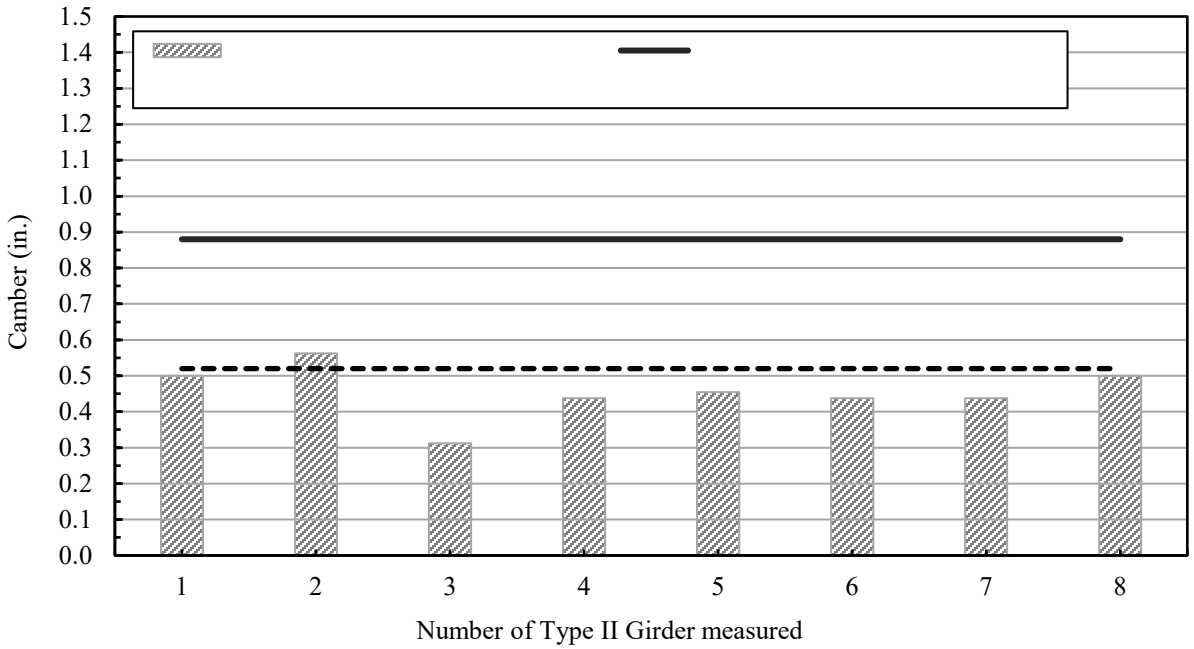

Figure 5-6. Comparison of the measured, the design erection camber, and the predicted camber using the recommended method for AASHTO Type II girders.

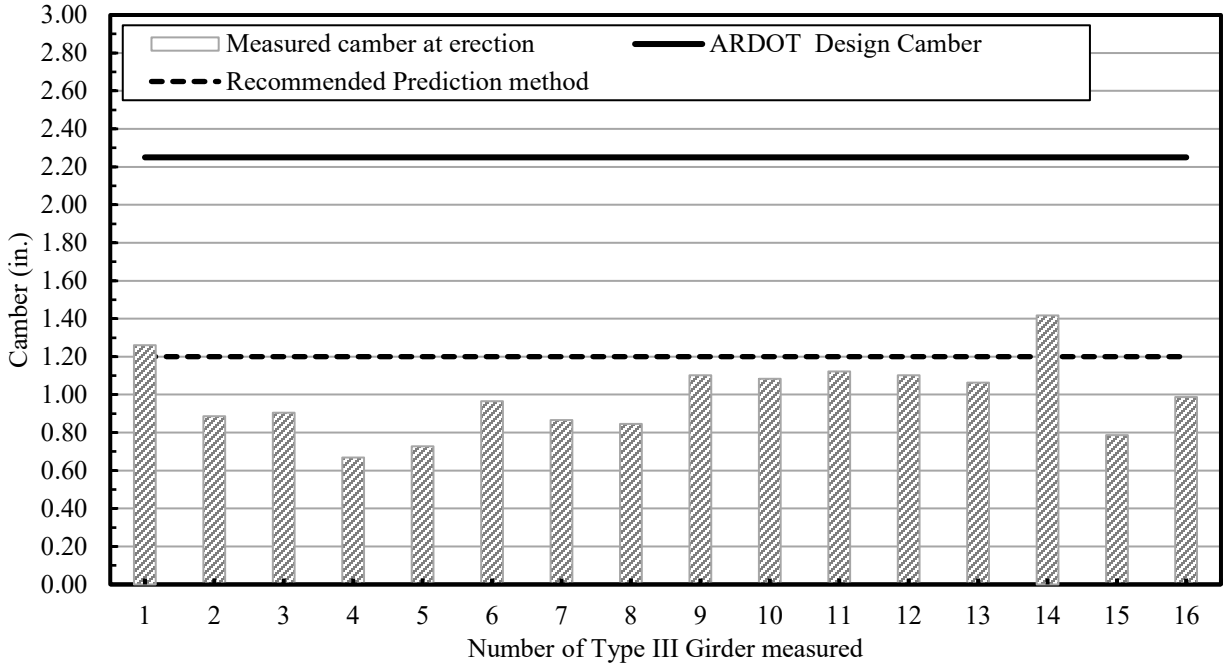

Figure 5-7. Comparison of the measured, the design erection camber, and the predicted camber using the recommended method for AASHTO Type III girders.

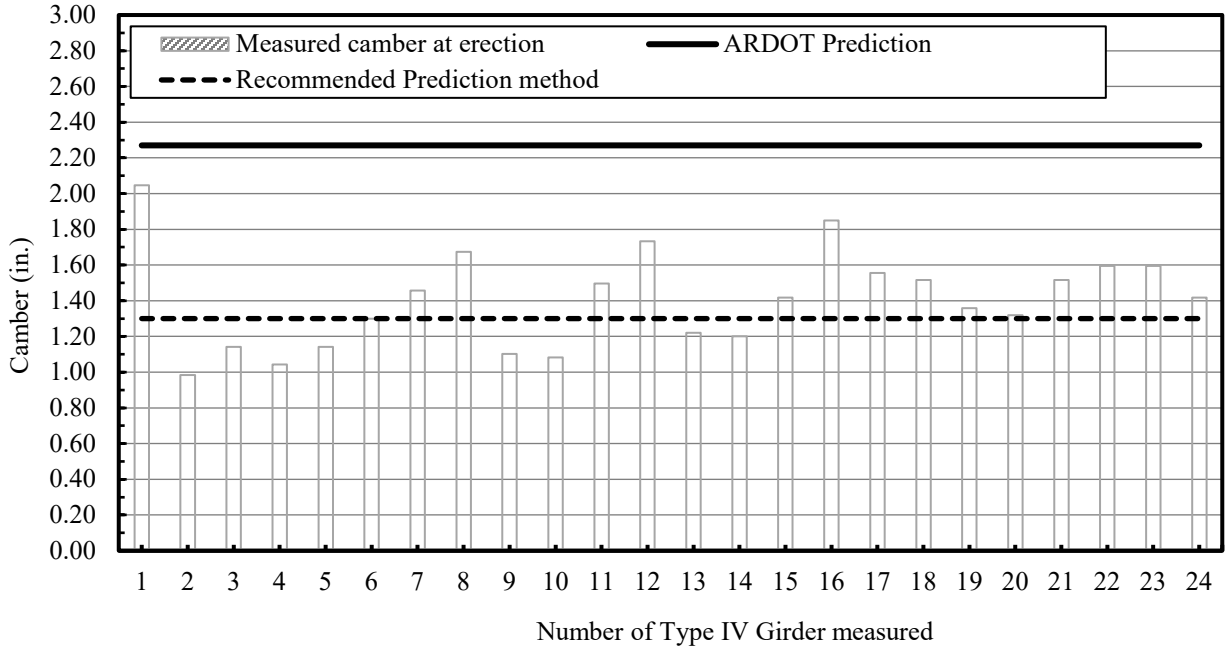

Figure 5-8. Comparison of the measured, the design erection camber, and the predicted camber using the recommended method for AASHTO Type IV girders.

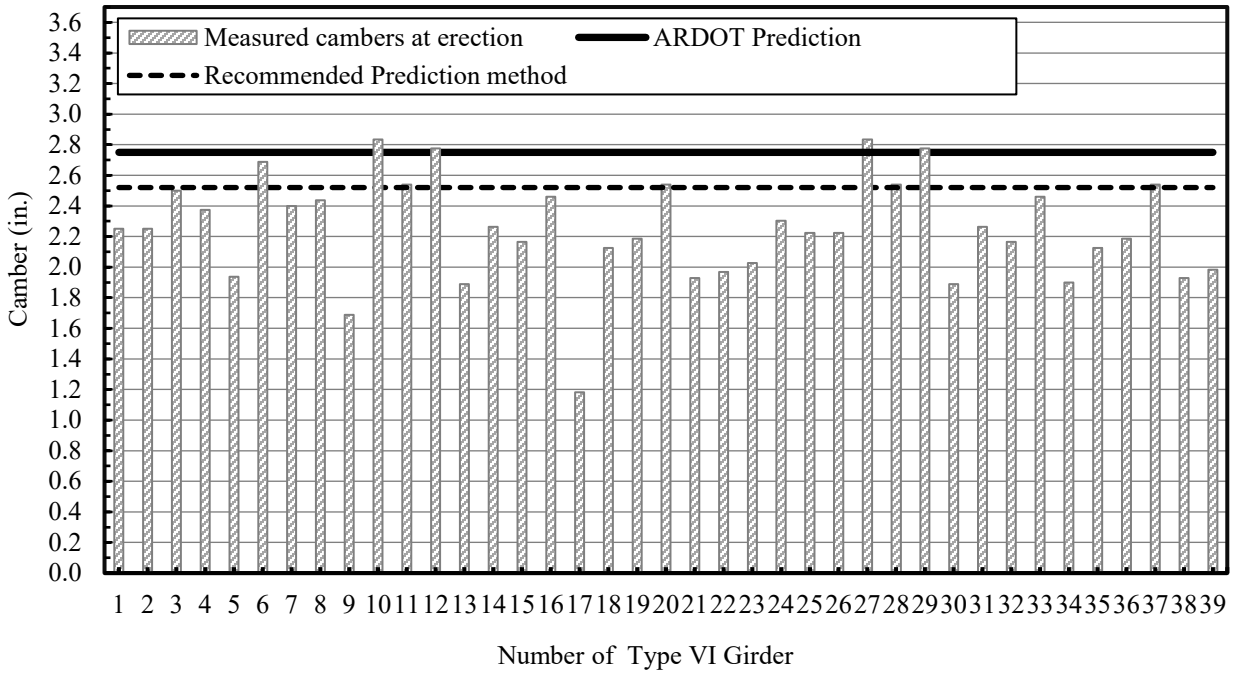

Figure 5-9. Comparison of the measured, the design erection camber, and the predicted camber using the recommended method for AASHTO Type VI girders.

4.5 Design Versus Measured Initial Camber

Unlike the camber at erection, the initial camber can be calculated with relative accuracy since the elastic modulus and the elastic shortening loss are affected by controlled conditions. However, for short girders, the measured initial camber was 53% and 39% less than the design values for AASHTO Type II and Type III girders, respectively. This is attributable mainly to the higher concrete compressive strength at release. The measured concrete strength was 66% higher than the design strength which increased the girder stiffness, and consequently, reduced the initial camber. The design initial camber was closer to the measured for AASHTO Type IV and VI girders as shown in Figure 5-10 below.

It was determined that the initial camber measured on the prestressing bed was less than that measured after moving the girder to the storage yard. The friction between the girder ends and the bed prevented full cambering and gives a false reading for the initial camber. The effect of the friction on the initial camber measurements was confirmed by other researchers (Honarvar et al., 2015; Ward 2010). The friction effect is neither consistence nor predictable. For three Type

VI girders, the camber measured on the prestressing bed was 50%, 35%, and 8% less than the cambers for the same girders measured in the storage yard. Therefore, the initial camber should be measured as soon as the girders are moved to the storage yard.

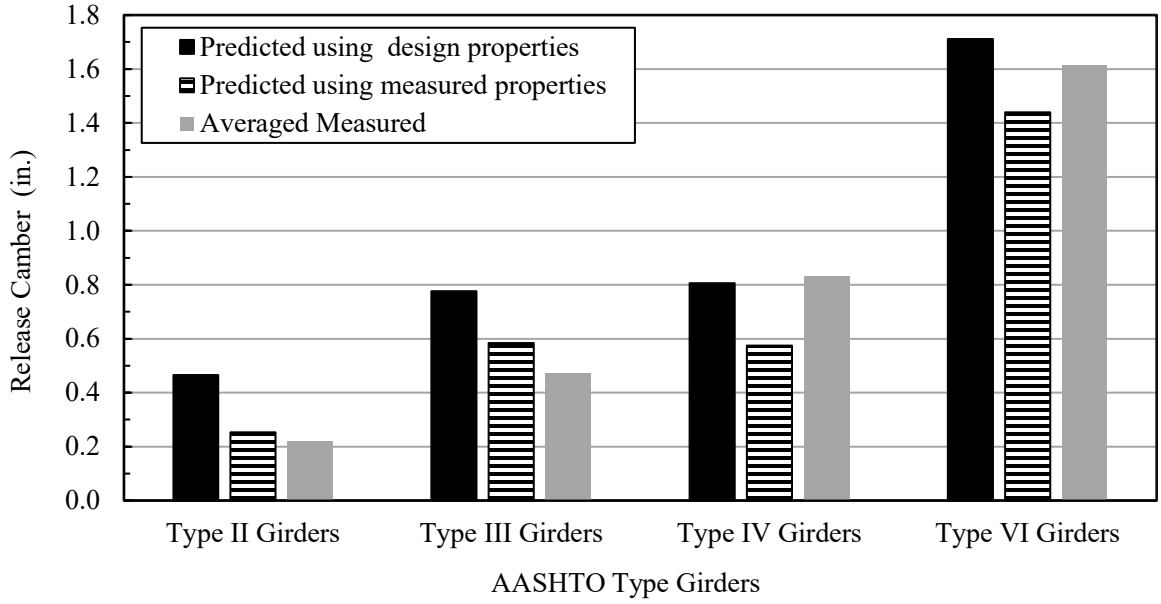

Figure 5-10. Comparison of the averaged measured release camber with the design and the predicted values

4.6 Evaluation of the Deflection at Deck Placement

Limited data are available for evaluating the deflection of prestress concrete bridge girders due to deck placement. Most research that aimed to improve camber prediction did not consider camber change due to the self-weight of the deck. In this study, camber was measured at each bridge site before and after deck placement to quantify the elastic deflection. Checking the elastic deflection may not be required in the specification. However, long-term deflection should be evaluated to ensure that the structure does not develop excessive deflection. In an attempt to quantify the long-term creep deflection, camber measurements were taken for some existing bridge girders that were in service. The results revealed deflections that reached up to 0.7 in. in the existing Type III girders.

Mid-span deflection was calculated using basic structural analysis. The concrete deck weight was assumed to be uniformly loaded over a simply supported beam. For AASHTO Type II and III

girders, deflection was measured by calculating the difference in camber before and after deck placement. Before casting the deck, camber elevation was measured at three points along the girder's top flange. After casting the deck, camber was measured under the bridge on the bottom surface of the bottom flanges. For the AASHTO Type VI girders, deflections were measured using two benchmarks for each span, and the elevation of the bottom flange at mid-span was recorded before and after deck casting. Deflection was the difference in the two elevations.

Figure 5-11 compares the measured deflections with the design values. The girders deflected much less than expected which may be attributed to two main reasons. First, the actual concrete compressive strength was greater than expected. This increased girder stiffness and in turn decreased deflection. Second, the girders were laterally restrained at the ends and at mid-span before deck placement. This restraint made the girders deflect as a group, which increased the rigidity of the system (Tadros et al. 2011). As shown in Figure 5-11, the measured deflections of the AASHTO Type II and III girders were less than the predicted values determined from either design procedure. Using the actual concrete properties (the "Proposed Predicted" values), improved the accuracy of the estimate, but the measured deflection was still less than the estimated value. Therefore, it is recommended to reduce the calculated deflection for short girders by a factor of 0.5. For AASHTO Type VI girders, using the modified concrete properties (proposed in Section 6.3), improves the estimation of the elastic deflection at deck placement. In general, having deflection less than the expected is not considered a performance related problem for bridge girders, especially when there is not enough camber at erection as in the case of Type II and III girders. The remaining camber after deck placement is necessary to compensate for the long-term creep deflection.

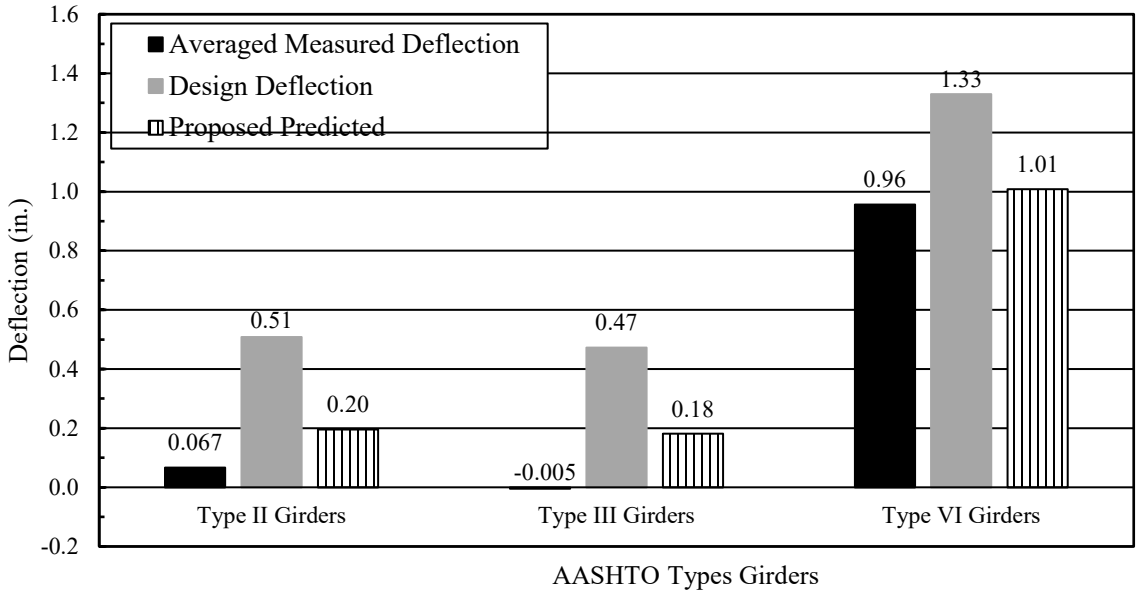

Figure 5-11. Comparison of the measured, the designed, and the predicted deflection using the recommended method for AASHTO Type II girders.

4.7 Prestress Loss Measurements

By measuring strain in the prestressing strands, one can determine the actual prestressing force in the strands which affect the camber of the prestressed girders. Researchers (Woolf and French, 1998) found that camber can change by 10% to 16% for each 5% change in the prestressing force. Measuring strand strain and therefore strand stress will not only improve camber prediction, but with knowing strand stress, one can also evaluate and calibrate the prestress losses prediction methods. An accurate estimate of prestress losses is necessary to evaluate concrete stresses and deformations under service conditions (Al-Omaishi et al. 2009). In this research project, vibrating wire strain gages were embedded in nine prestressed concrete bridge girders, which were used in three bridges within the state of Arkansas. The strain gauges were placed after tensioning the strands and before placing the concrete. One gauge was attached to the bottom strands and a second gauge was attached to the top stands. In addition to providing strain data, these gauges also recorded concrete temperature. Concrete temperature was recorded to monitor the hydration temperature and thermal gradient within the girder.

4.7.1 Total prestress losses at deck placements

The measured prestress losses and the predicted (or design) prestress losses are shown in Figure 5-12. For all girders at deck placement, the measured prestress losses were less than the predicted values obtained using the Refined Method in the 2014 AASHTO LRFD bridge code. As shown in Figure 5-12, the percent differences between the measured and predicted prestress losses at the time of deck placement is 59%, 46%, 46%, and 12% for AASHTO Type II, III, IV, and VI girders respectively. Although the deck has not been placed for the bridge with Type IV girders, the strand strain recorded at an age of 180 days from the casting day is assumed to be the strain reading at deck placement.

One of the reasons that led to the overestimation in the prestress losses is that the designers use the minimum concrete strength specified in design while the actual strength can be higher. It was determined that the 2014 AASHTO LRFD Refined Method overestimates the total prestress losses at the time of deck placement, especially for the AASHTOO Type II and III girders. Camber prediction and prestress losses prediction at any point during construction are directly related to the concrete properties at that stage. Also, predicted camber at the time of deck placement is further complicated because of the differences between measured and predicted prestress losses.

Data from the field monitoring for the strands strain indicate that the 2014 AASHTO Refined Method overestimates the total prestress losses for short prestressed concrete girders. When using the measured concrete properties including the concrete elastic modulus, unit weight, time at release and time at deck placement, the Refined Method predicts losses that are approximately 42.7% and 24.7% more than the measured for girders Type II and Type III respectively. For the longer girders, the design prestress losses for Type IV and VI girders were 18.5% and 5.7% higher than the measured.

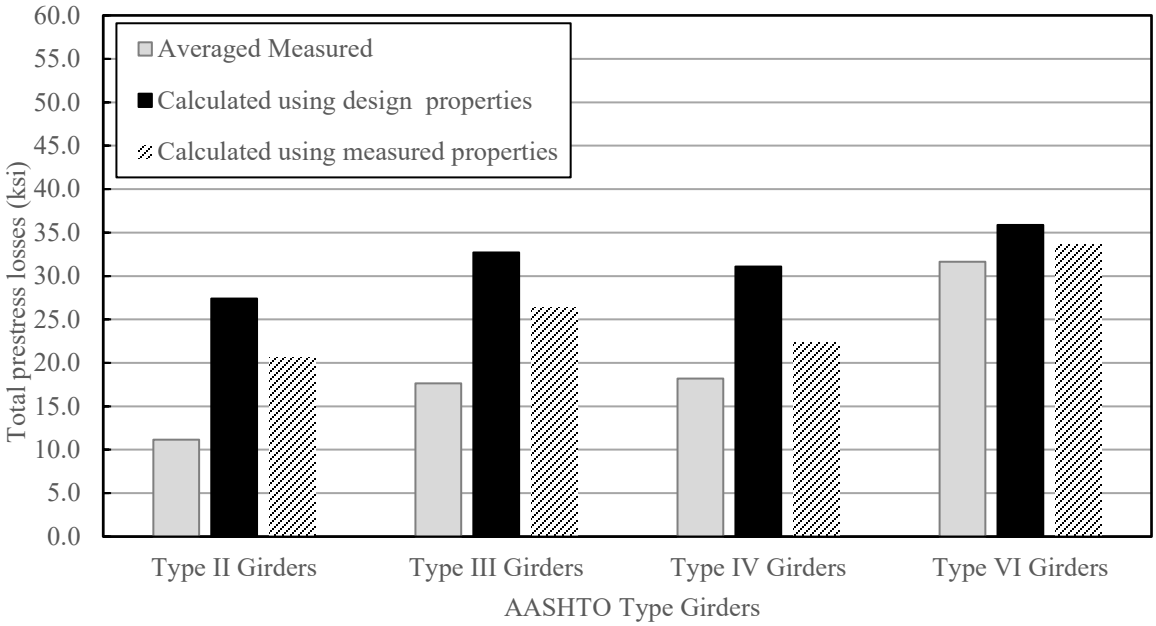

Figure 5-12. Comparison between the design and the measured total losses at deck placement.

4.7.2 Initial Prestress Losses

The predicted elastic shortening losses were closer to the measured values than the total prestress losses. The elastic shortening loss depends mainly on the modulus of elasticity of concrete at the time of release. If the concrete elastic modulus is accurately predicted, the elastic shortening loss should be close to the design value. Based on the measured strand strain, the error in the predicted elastic shortening loss ranged from -11% to 20.3% when compared to the measured values. When the actual concrete properties were used in the computation, the measured elastic shortening loss were higher than the design by 2% to 21.8%. This indicates that the AASHTO LRFD method underestimated the elastic shortening losses which was also found in a previous study (Barr et al., 2008). This error can be explained from the fact that the measured losses at release includes not only the elastic shortening loss, but also strands relaxation loss, anchorages slip loss, and seating loss. It is worth mentioning that the friction between the girder ends and the prestressing bed partially restrain the transfer of the prestressing force. A slight increase in the strand strain was observed after moving the girders off the bed. (Ward, 2010) found that a better estimate for elastic shortening is the loss that occurs after 5 hours from

release in a study conducted on Double Tee, prestressed concrete girders. Figure (5-13) compares the measured elastic shortening loss with the design values.

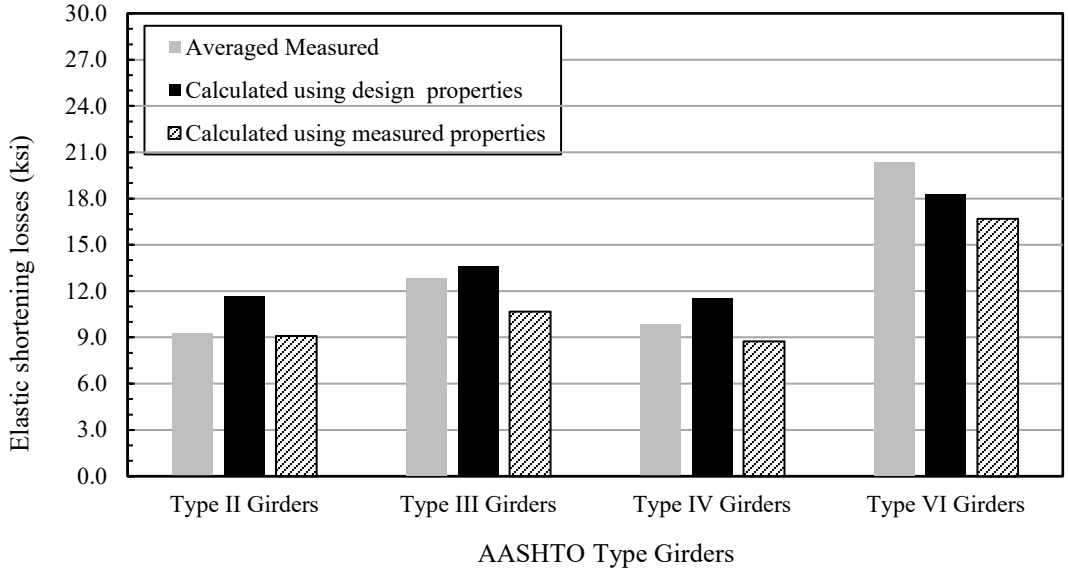

Figure 5-13. Comparison the design and the measured elastic shortening losses

In order to predict the prestress losses accurately, concrete properties should be estimated properly at the design stage. Therefore, the research team suggested using the recommendations discussed in Section 6.3 of this Report to estimate concrete properties. A more accurate estimate for prestress losses will also result in a more accurate estimate for camber and deflection prediction.

CHAPTER SIX

Comparison of Calculated and Measured Concrete Properties

5.1 Compressive Strength

More than 30 cylinders and 6 prisms were prepared from the concrete used to cast each type of the AASHTO girders. The concrete cylinders were 4 by 8 in. specimens. Concrete was collected from each girder on the prestressing bed when possible and from at least three different mixers. This was done in order to make the specimens more representative of the concrete, which comprised each girder. Test results indicated that the measured compressive strength for all girders was higher than their design strength. At the Coreslab Structures Inc. plant, the concrete compressive strength at release for the Type II, III, and VI girders were 27% to 73% higher than the design value. For Type IV girders, that were manufactured at the J.J. Ferguson Prestress-Precast Co., Inc. plant, the measured concrete strength at release was 59% higher than the design strength. The compressive strength at release directly impacts the camber at girder erection. Figure 6-1 shows a comparison between the design and measured compressive strength at release. At 28 days of age, the average measured compressive strength at both plants was 69% percent higher than the design strength (Figure 6-2).

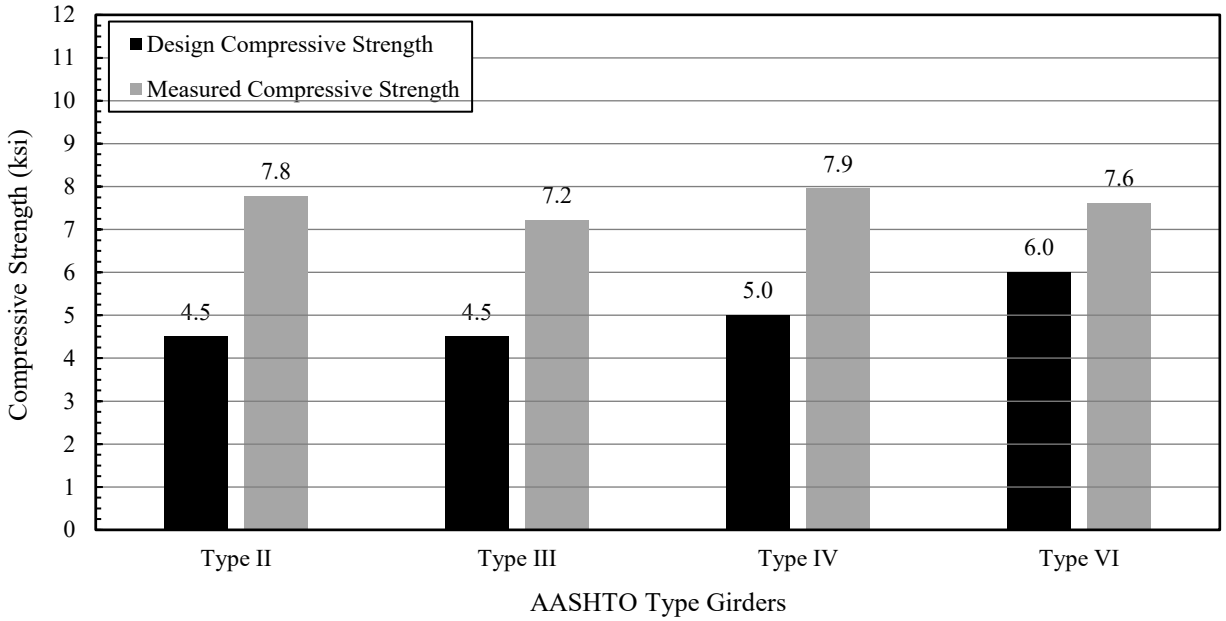

Figure 6-1. Comparison of the measured to the design concrete compressive strength (ksi) at release.

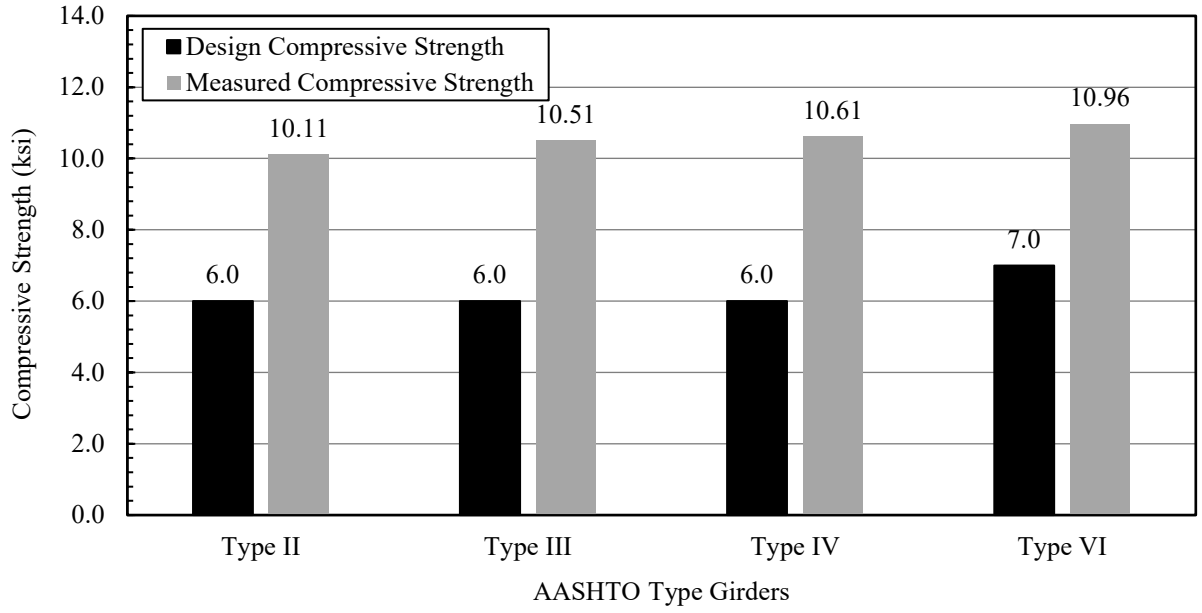

Figure 6-2. Comparison of the measured to the design concrete compressive strength (ksi) at 28 days.

The study found that both plants produced concrete with higher compressive strengths than the design value. The reason for this is to obtain the required design strength as early as possible.

This allows the plant to release strands earlier and move the girders out of the precasting bed, which allows the plant to decrease production time. Typically, one of the goals of the precasters is to maintain a 24-hour production cycle. Failure to obtain the design release strength in time will affect the daily work schedule since strands cannot be released until the concrete achieves the specified release strength.

5.2 Modulus of Elasticity

As compressive strength increases, the elastic modulus also increases which in turn increases girder stiffness. As shown in Figure 6-3, the modulus of elasticity (MOE) at release was 15% to 44% higher than the design values when using the AASHTO LRFD equation (Eq. (2-36) and the specified compressive strength to estimate MOE. When using the ACI equation (Eq. (2-37)) for estimating MOE, the measured values were 25% to 53% higher than the predicted values. As concrete and therefore girder stiffness increases, camber and deflection are less than expected. This also affects prestress losses, which will also be less than predicted.

$$E_c = 33000 K_1 w_c^{1.5} \sqrt{f_c'} \quad (2\text{-}36)$$

$$E_c = \left[1000 + 1265\sqrt{f_c'}\right] \left(\frac{W_c}{0.145}\right)^{1.5} \quad (2\text{-}37)$$

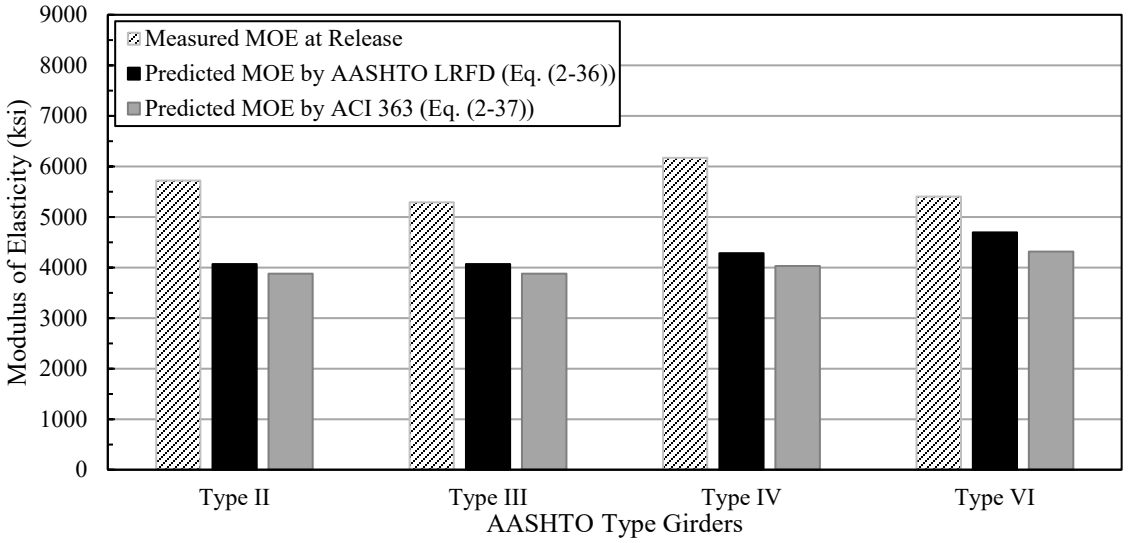

Figure 6-3. Comparison of the measured and predicted modulus of elasticity at release.

5.3 Recommended Prediction for Concrete Compressive Strength

When the concrete compressive strength is higher than the design value, all the predicted parameters that incorporate compressive strength will be affected. To account for this difference, the authors recommend the following: 1) Assume the compressive strength at release is equal to 7.2 ksi when the design value is below 7.0 ksi. 2) Assume the compressive strength at release is 10% higher when the design value is 7.0 ksi and above. 3) Assume the concrete compressive strength at 28 days and at later ages is 50% higher than the design value. 4) Use the 2014 AASHTO LRFD equation to predict the MOE with the appropriate K_1 factor from Table 6-2. 5) Assume the girder age at deck placement is 180 days. Implementation of these recommendations will improve the accuracy of predicting camber, deflection, and prestress losses.

5.4 Observed Shrinkage Strain Behavior

As stated in section 4.2, two procedures were followed in curing the shrinkage test specimens. For each girder type, six concrete prisms were sampled. Three prisms submerged in lime-saturated water for 28 days followed by air drying according to the ASTM C 157/C 157M, and the other three were demolded, their initial comparator readings recorded, and then stored directly in a drying room at a temperature of 73 ± 3 °F. For all test specimens, the shrinkage strain was monitored for more than a year. However, to obtain consist comparison between test specimens, all data in Figure 6-4 below corresponds to a shrinkage strain at an age of approximately 360 days.

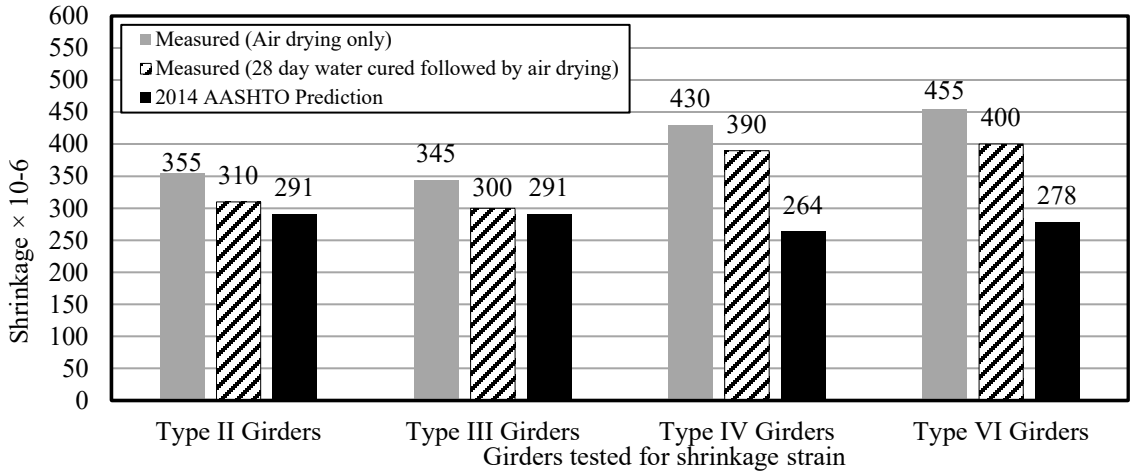

Figure 6-4. Comparison of the measured and predicted shrinkage strain at age of 1 year.

For the prisms sampled from Type II and Type III girders, the measured shrinkage strains were close to the predicted value found by using the 2014 AASHTO LRFD specification as shown in Figure 6-4. However, for the Type IV and VI girders, the measured shrinkage strain was 48% and 44% larger than the predicted values, respectively. The reason for these discrepancies may be attributed to the curing methods. Type II and Type III girders were heat cured for 13 to 16 hours which reduced the shrinkage strain, while Type IV and VI girders were not subjected to heat curing. It is expected that shrinkage for Type II, and III girders would be higher than the predicted values if they had not been subjected to steam curing. It should be noted that the Type II, III, and VI girders have the same mixtures proportions which eliminates any differences that could occur due to the effect of cement and water content. Therefore, it can be concluded that AASHTO LRFD procedure underestimates concrete shrinkage. Test results also indicate that the measured shrinkage strain for the specimens subjected to initial wet curing was closer to the design than strain for the specimens stored without water curing. Early drying for the prisms increased the shrinkage strain by 13% on average comparing to those submerged in water for 28 days.

5.5 Observed Creep Strain Behavior

The creep strain was monitored for two representative concrete mixtures from the Coreslab Structures Inc. plant and the J.J. Ferguson Prestress-Precast Co., Inc. plant. Note that the

shrinkage strain was subtracted from the total strain for the sealed and the unsealed specimens. After the initial load had been applied, the elastic strain was recorded, and the creep strain has been monitored. The goal is to monitor the creep strain for one year to be used in future research. Figure 6-5 compares the total creep strain for the sealed and unsealed cylinders. The total stain shown in Figure 6-5 was recorded for up to six months from the loading day. Additional descriptions of the creep test frame, loading procedure, and strain measurements were given in Section 4.3.

Few observations can be made from creep test results. The total strain for the unsealed specimens was 6.2 % higher than that for the sealed specimens. The reason is sealing the cylinders prevents moisture movements from and into the cylinders which minimizes the microcracking and reduces the strain. Epoxy sealing also prevents moisture loss and reduces the drying shrinkage. Table 6-1 compares the creep coefficients for the sealed and unsealed specimens with the design values calculated according to the 2014 AASHTOO LRFD specification. The measured creep coefficients for the sealed specimens are closer to the design values than the creep coefficients for the unsealed. Unsealed cylinders have higher creep coefficient as they have higher shrinkage and creep strain.

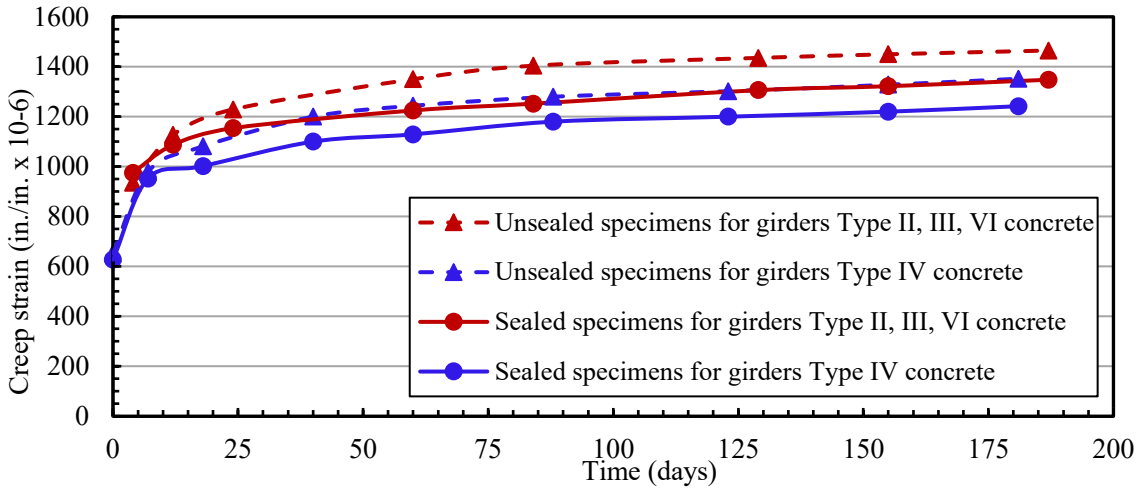

Figure 6-5. Creep strain versus time for two concrete mixtures used in casting the girders.

Table 6-1. Measured Creep coefficient compared to the design by 2014 AASHTO Specification.

	Measured unsealed	Measured sealed	Predicted
Concrete mixture for girders Type II, III, and VI	1.0	0.91	0.89
Concrete mixture for girders Type IV	1.0	0.90	0.85

5.6 Improving the Prediction of Modulus of Elasticity

The MOE of concrete or any other material is a measure of its stiffness. It is the ratio of the applied stress to the corresponding instantaneous strain within the linear portion of the stress-strain curve. Since the MOE is the slope of the elastic (linear) portion of the stress strain curve, it can indicate how much stress the concrete can resist without having permanent deformation. Therefore, the MOE of the concrete is very important property in computing the maximum allowable design stress, moment, and deflection.

Concrete is not a homogenous material. It consists mainly of two components (cement paste and coarse aggregate) that have different elastic modulus. The existence of the interfacial transition zone between the paste and coarse aggregate makes concrete a even more complex material. The MOE of concrete is influenced by the strength and porosity of the above three components. Since density is directly related to material porosity, most empirical expressions used to calculate the MOE of concrete assume a direct relationship to compressive strength and unit weight of concrete (Mehta and Monteiro 2013).

In the design of prestressed concrete girders, accurate prediction of the elastic modulus is necessary when calculating camber and prestress losses (Tadros et al., 2003; Barr et al., 2009). The prediction of camber and deflection are influenced by the accuracy of the estimated elastic modulus. Equation (5.4.2.4-1) in 2014 AASHTO LRFD, referred herein as Eq. (2-36), accounts for the effect of coarse aggregate type by the factor, K_1. In the NCHRP Report 496, Tadros et al. found the K_1 values for coarse aggregates in five different states. The K_1 values, which is the ratio of predicted to measured modulus of elasticity, were 1.037, 1.122, 0.768, and 0.889 for aggregate collected from Nebraska, New Hampshire, Texas, and Washington respectively. Barr et al., 2009

conducted a study aimed to improve the prediction of prestress losses for UDOT. The K_1 value was found to be 0.896. In this study, the K_1 values were also determined by dividing the measured MOE by the predicted value from Eq. (2-36) using the corresponding compressive strength for each mix. Figures (6-6) through (6-8) show the MOE plotted against the compressive strength. These figures also show K_1 values with the improved prediction for the elastic modulus.

$$E_c = 33000 K_1 w_c^{1.5} \sqrt{f_c'} \qquad (2\text{-}36)$$

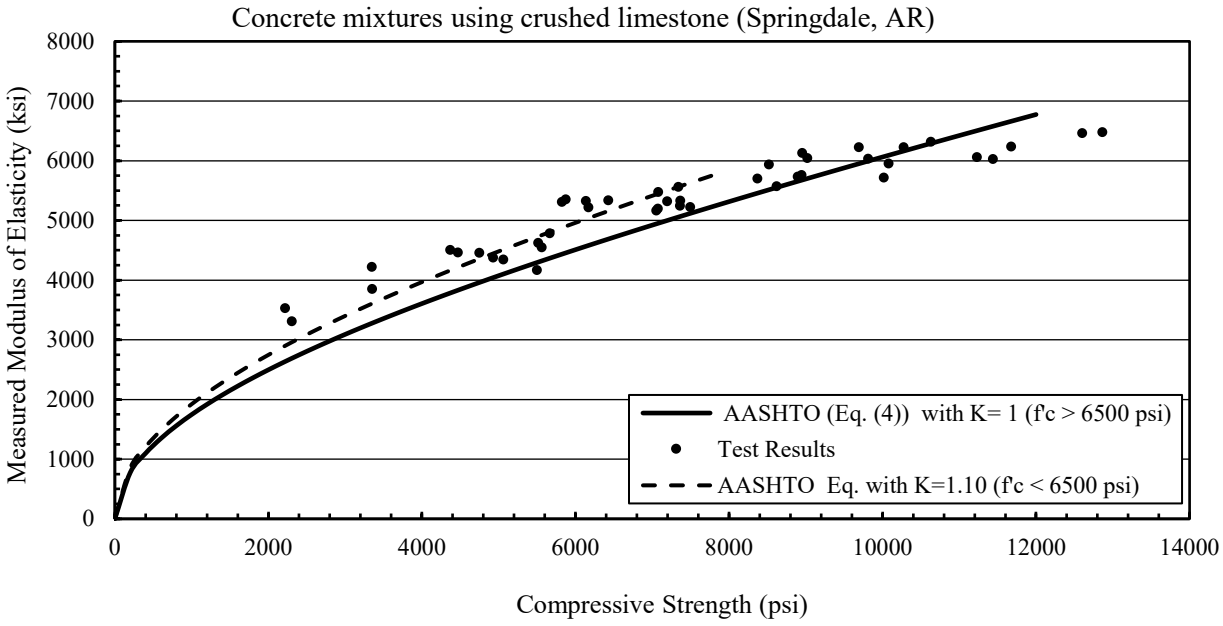

Figure 6-6. The experimental results of modulus of elasticity for concrete mixed with crushed limestone from Springdale, AR. compared to the predicted.

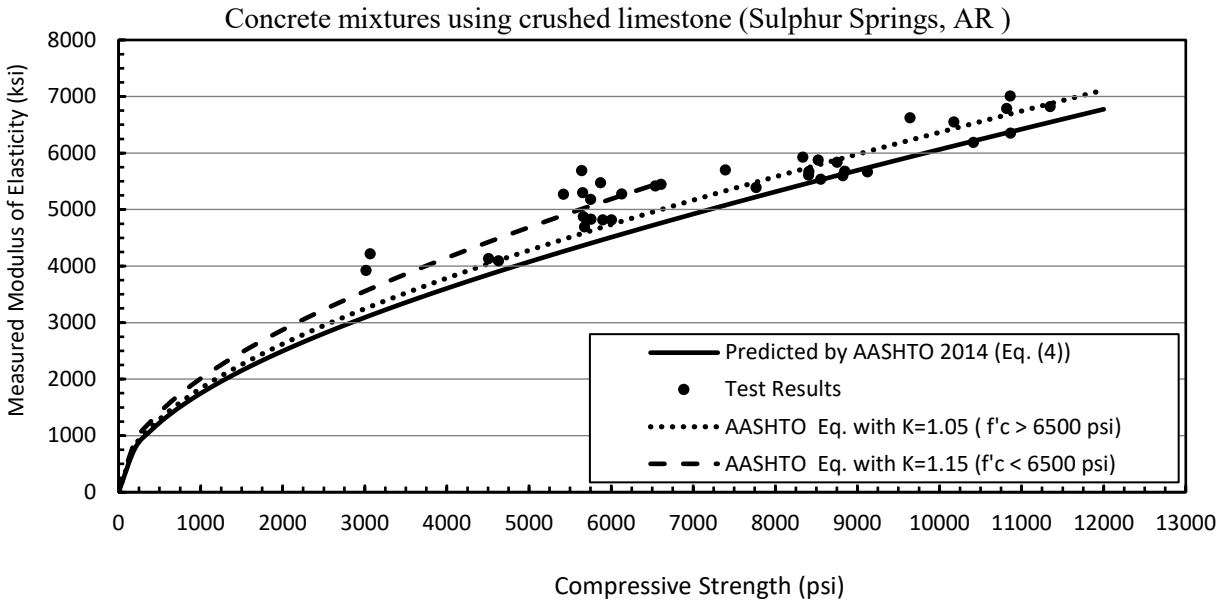

Figure 6-7. The experimental results of modulus of elasticity for concrete mixed with crushed limestone from Sulphur Springs, AR. compared to the predicted.

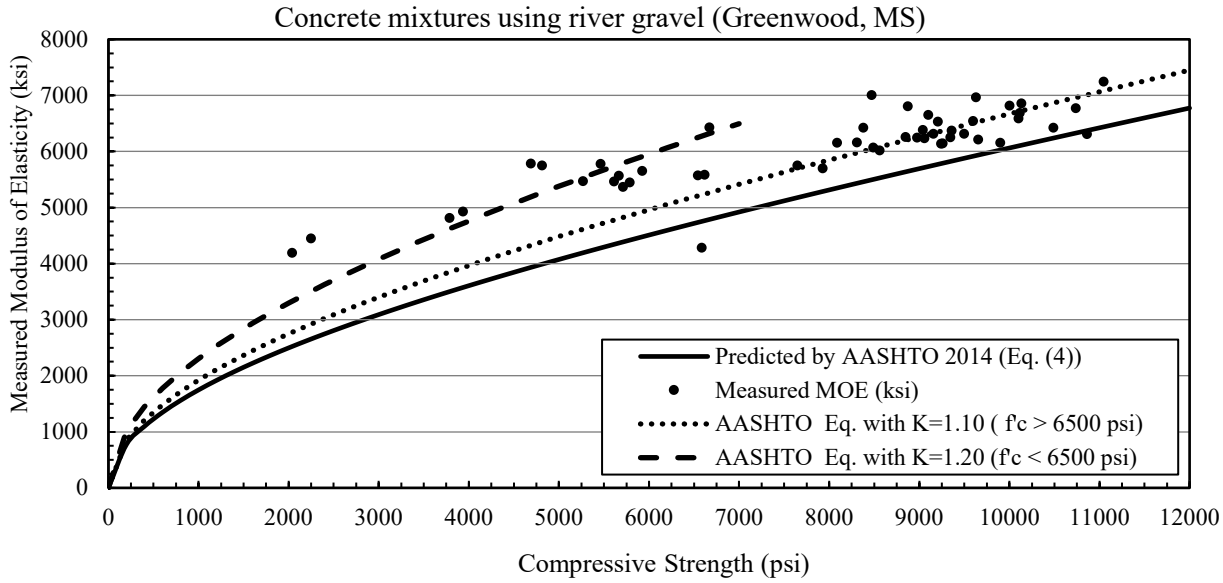

Figure 6-8. The experimental results of modulus of elasticity for concrete mixed with river gravel from Greenwood, MS. compared to the predicted.

The AASHTO LRFD (2014) equation predicts a closer estimate for the MOE when the concrete compressive strength is greater than 6500 psi. Therefore, it was more realistic to derive two K_1

coefficients with an applicable range below and above 6500 psi. K_1 coefficients shown in Figures (6-6) through (6-8) are summarized in Table 6-3 below.

Table 6-2. Ratio of predicted to measured modulus of elasticity, K_1, for each type of aggregate

Range of Applicability	Crushed limestone (Sulphur Springs, AR)	River Gravel (Greenwood, MS)	Crushed limestone (Springdale, AR)
$f'_c < 6.5$ ksi	1.15	1.20	1.10
$f'_c > 6.5$ ksi	1.05	1.10	1.00

CHAPTER SEVEN

Summary, Conclusions, and Recommendations

6.1 Summary

This report confirmed that an update or modification to the current prediction method of long-term camber and deflection in prestressed concrete bridge girders is needed. Several state departments of transportation have developed their own camber prediction methods. This is due to girders having cambers that are less than expected. This research project investigated the performance of girders fabricated at two precast prestressed concrete plants, Coreslab Structures Inc. plant in Tulsa, OK and J.J. Ferguson Prestress-Precast Co., Inc. plant in Greenwood, MS. These plants produce the majority of the prestressed concrete bridge girders used in the state of Arkansas. Field measurements for camber and strand stress along with extensive concrete material tests were conducted through several trips to the precast plants and two bridge construction sites. The study involved nine AASHTO Types girders of different lengths and cross sections.

6.2 Conclusion

After two years of taking measurements from the time of casting to the completion of the bridge, the following conclusion are made:

1. The current method that the ARDOT uses overestimates camber, specifically in the AASHTO Type II and III girders.
2. The measured camber at erection for all girders is less than the design camber by 93%, 128%, and 25% for the AASHTO Type II, III, and VI girders, respectively. The over estimation in camber can be attributed to the actual concrete compressive strength at release being greater than the design strength.
3. The actual concrete compressive strength is greater than the specified compressive strength. Girder producers intentionally over design the concrete mixtures to achieve enough compressive strength for release in less than 24 hours. This optimizes productivity and maintains consistent working schedules.

4. The measured modulus of elasticity of concrete is higher than the predicted because of the higher concrete compressive strength. In addition, the AASHTO LRFD (2014) tends to under estimate the elastic modulus by up to 20%.
5. After casting the concrete deck, all the girders involved in the study deflected less than the design value because of the higher modulus of elasticity and the lateral supports at the ends and at mid-span of the girders.
6. At the time of girder erection, prestress losses are less than the calculated values using the design concrete properties.
7. The refined method of estimating prestress losses in Section 5.9.5.4 of the 2014 AASHTO LRFD overestimates the total prestress losses at the time of deck placement for the AASHTO Type II and III girders.
8. The 2014 AASHTO LRFD Refined Method for estimating prestress losses provides a good estimate for the total prestress losses at the time of deck placement for AASHTO Type VI girders.
9. The AASHTO LRFD specification under estimates the shrinkage strain of concrete by up to 48% when compared with the measured values.

6.3 Recommendations:

1. Concrete compressive strength should be taken as:
   a) 7.2 ksi. at release when the specified compressive strength at release is less than 7.0 ksi.
   b) 10% higher than the specified compressive strength at release when the specified compressive strength at release is equal or greater than 7.0 ksi.

2. The current ARDOT bridge design specification should be adjusted to specify the 28^{th} day concrete compressive strength 50% higher than the design compressive strength at release.

3. The modulus of elasticity should be predicted according to the 2014 AASHTO LRFD equation. K_1 values provided in Table 6-3 should be used.

4. When estimating the initial camber at release camber, use the transformed section properties.

5. Camber at girder erection should be estimated as follows:

$$\Delta_{\text{erection camber}} = 1.4 \times \uparrow\Delta_{\text{initial}} \quad (2)$$

Where:

$\uparrow\Delta_{\text{initial}}$ = the initial camber at release calculated using the gross section properties.

1.4 = multiplier to account for the long-term growth in camber.

6. The contractor should update camber, deflection and the road longitudinal profile based on the measured concrete strength to decrease the discrepancy between the design and the actual cambers. More effectively, the fabricators can provide the contractor with the average camber values for the girders in the storage yard and update the road profile accordingly. However, camber should still be estimated based on the recommended procedure so that adjustment for the camber and deflection may not be needed.

7. Girders should be cast based on a scheduled erection plan to minimize storage time and to reduce the effect of creep and shrinkage on camber prediction.

8. The recommendations for predicting concrete compressive strength and modulus of elasticity should be utilized when estimating deflection due to the cast-in-place deck weight. Following this procedure leads to a conservative deflection estimation because all the girders included in the study deflected less than predicted.

9. The initial camber and the elastic shortening losses should be measured after moving the girder to the storage yard to eliminate the effect of the friction from the prestressing bed on camber.

References

(AASHTO) American Association of State Highway and Transportation Officials. (2005). *AASHTO LRFD bridge design specifications - SI units* (5th ed.). Washington, DC: AASHTO.: Association of State Highway and Transportation Officials.

(ACI 318-08). (2008). *Building code requirements for structural concrete and commentary*. Farmington Hills, MI: American Concrete Institute.

ACI Committee 209-92. (2008). Guide for modeling and calculating shrinkage and creep in hardened concrete.

ACI Committee 363. (1992). *State-of-the-art report on high strength concrete*. Detroit, MI:

Ahlborn, T. M., French, C. E., & Shield, C. K. (2000). High-strength concrete prestressed bridge girders: Long term and flexural behavior.

Aïtcin, P., & Mehta, P. K. (1990). Effect of coarse aggregate characteristics on mechanical properties of high-strength concrete. *Materials Journal, 87*(2), 103-107.

Al-Omaishi, N., Tadros, M. K., & Seguirant, S. J. (2009a). Elasticity modulus, shrinkage, and creep on high-strength concrete as adopted by AASHTO. *PCI Journal, 54*(3)

Al-Omaishi, N., Tadros, M. K., & Seguirant, S. J. (2009b). Estimating prestress loss in pretensioned, high-strength concrete members. *PCI Journal, 54*(4)

American Association of State Highway and Transportation Officials, (AASHTO). (2014). *AASHTO LRFD bridge design specifications - SI units* (7th edition). Washington, DC: AASHTO.

ASTM C157/C157M-17. (2017). *Standard test method for length change of hardened hydraulic-cement mortar and concrete*. West Conshohocken, PA://doi.org/10.1520/C0157_C0157M-17

ASTM C39/C39M-18. (2018). * standard test method for compressive strength of cylindrical concrete specimens*. West Conshohocken, PA: ASTM International.//doi.org/10.1520/C0039_C0039M-18

ASTM C512/C512M-15. (2015). * standard test method for creep of concrete in compression*. West Conshohocken, PA: ASTM International.//doi.org/10.1520/C0512_C0512M-15

ASTMC469/C469M−14. (2014). *Standard test method for static modulus of elasticity and poisson's ratio of concretein compression*. West Conshohocken, PA: ASTM International.//doi.org/10.1520/C0469_C0469M

Barr, P. J., Kukay, B. M., & Halling, M. W. (2008). Comparison of prestress losses for a prestress concrete bridge made with high-performance concrete. *Journal of Bridge Engineering, 13*(5), 468-475. 5(468) Retrieved from http://ascelibrary.org/doi/abs/10.1061/(ASCE)1084-0702(2008)13:5(468)

Barr, P. J., Halling, M., Boone, S., Toca, R., & Angomas, F. (2009). UDOT's Calibration of AASHTO's New Prestress Loss Design Equations. *Utah Department of Transportation Research Division, Final Report*

Cook, R. A., Bloomquist, D., & Sanek, J. E. (2005). *Field verification of camber estimates for prestressed concrete bridge girders.* (). Gainesville - Florida: University of Florida.

Honarvar, E., Nervig, J., He, W., Sritharan, S., & Rouse, J. M. (2015). *Improving the accuracy of camber predictions for precast pretensioned concrete beams.* (Final Report). Ames, IA:

Martin, L. D. (1977). A rational method for estimating camber and deflection of precast prestressed members. *PCI Journal, 22*(1), 100-108.

Mehta, P. K., & Monteiro, P. J. M. (2013). *Concrete: Microstructure, properties, and materials* (4th ed. ed.). New York: McGraw-Hill Professional. Retrieved from http://lib.myilibrary.com?ID=544221

Nguyen, H., Stanton, J., Eberhard, M., & Chapman, D. (2015). The effect of temperature variations on the camber of precast, prestressed concrete girders. *PCI Journal, 60*(5), 48-63. 10.15554/pcij.09012015.48.63

Nilson, A. H. (1987). *Design of prestressed concrete* (second edition edition). Ithaca, New York: Wiley.

Noguchi, T., Tomosawa, F., Nemati, K. M., Chiaia, B. M., & Fantilli, A. P. (2009). A practical equation for elastic modulus of concrete. *ACI Structural Journal, 106*(5), 690.

O'Neill, C., & French, C. (2012). Validation of prestressed concrete I-beam deflection and camber estimates. *Final Report*, 26-99.

PCI design handbook. (2010). *PCI design handbook: Precast and prestressed concrete* (7th edition). Chicago, IL.: Precast/Prestressed Concrete Institute, (PCI).

Precast/Prestressed Concrete Institute. (2014). * bridge design manual* (3rd Second Release, ed.). Chicago, IL: Precast/Prestressed Concrete Institute (PCI).

Rizkalla, S., Zia, P., & Storm, T. (2011). *Predicting camber, deflection, and prestress losses in prestressed concrete members* (Final Report). Raleigh, NC: North Carolina State University.

Rosa, M. A., Stanton, J. F., Eberhard, M. O., Khaleghi, B., & Engineer, B. D. (2007). *Improving predictions for camber in precast, prestressed concrete bridge girders* (Final Research Report). Seattle, Washington: Washington State Department of Transportation.

Stallings, J. M., & Eskildsen, S. (2001). *Camber and prestress losses in high performance concrete bridge girders.* (). Auburn, AL: Alabama Department of Transportation.

Storm, T. K., Rizkalla, S. H., & Zia, P. Z. (2013). Effects of production practices on camber of prestressed concrete bridge girders. *PCI Journal, 58*(1)

Tadros, M. K., AL-Omaishi, N., Seguirant, S. J., & Gallt, J. G. (2003). *Prestress losses in pretensioned high-strength concrete bridge girders.* (project 18-07 report 496.). Washington, D.C.: National Cooperative Highway Research Program (NCHRP).

Tadros, M. K., Fawzy, F. F., & Hanna, K. E. (2011). Precast, prestressed girder camber variability. *PCI Journal, 56*(1), 135-153.

Tadros, M. K., Ghali, A., & Meyer, A. W. (1985). Prestressed loss and deflection of precast concrete members. *PCI Journal, 30*(1), 114-141. 10.15554/pcij.01011985.114.141

Ward, D. (2010). *Performance of prestressed double-tee beams cast with lightweight self-consolidating concrete* (PhD. Thesis) University of Arkansas.

Woolf, D., & French, C. (1998). A camber study of MnDOT prestressed concrete I-girders. *Final Report*